



**Politecnico
di Torino**

Master of Science in Mechanical Engineering

Master Thesis

Methodological Development for a Li-Ion Cell
Experimental and Virtual Characterization

Tutor

Prof. Davide Papurello

Candidate

Mohamed Hazem Ali Selim

بِسْمِ اللَّهِ الرَّحْمَنِ الرَّحِيمِ

(قُلْ إِنَّ صَلَاتِي وَنُسُكِي وَمَحْيَايَ وَمَمَاتِي لِلَّهِ رَبِّ الْعَالَمِينَ ** لَا شَرِيكَ لَهُ وَبِذَلِكَ أُمِرْتُ وَأَنَا أَوَّلُ الْمُسْلِمِينَ)

صَدَقَ اللَّهُ الْعَظِيمِ

سورة الأنعام (162,163)

(Say, "Indeed, my prayer, my rites of sacrifice, my living and my dying are for Allāh, Lord of the worlds, No partner has He. And this I have been commanded, and I am the first [among you] of the Muslims.)

Al An'am sourat (162,163)

((Di: "In effetti, la mia preghiera, i miei riti di sacrificio, la mia vita e la mia morte sono per Allāh, Signore dei mondi, nessun partner ha. E questo mi è stato comandato, e io sono il primo [tra voi] di I musulmani).)

Al An'am sourat (162,163)

Abstract

The interest in Lithium -Ion cells is constantly growing due to the increase of applications that benefit from such technologies, including the automotive industry, industrial machines and energy storage. The popularity of this technology derives from a series of advantages they possess: high energy density, lack of memory effect, safety and low maintenance. The performances of the Lithium -Ion battery (LIBs) are a lot influenced by the temperature of the environment and of the cell itself. In extreme temperatures, be cold that hot, in fact, phenomena are triggered that damage the capacity and durability of the battery and which can lead, in the most risky cases, to the explosion of the cell.

In recent years, many research studies have investigated to to develop a methodology for the experimental and virtual characterization of a Li-ion cell solutions that could make the batteries more efficient and safer in these operating conditions.

In this thesis, the goal is to model the thermal phenomena inside a Lithium -Ion cell and to simulate the a two dimensional thermal model to analyze the temperature distribution over the battery surface, using. Subsequently a multi-physical model on the Ansys Fluent and making the appropriate hypotheses with the thermal and electrical parameters which taken theoretically and experimentally.

Moreover, the thermal behavior of the battery has been investigated at different operating conditions (current rate) in charge and discharge.

Acknowledgments

My academic career ends. A period of life that has given me so much, from all points of sight: joy, fatigue, suffering, satisfaction. A period that has made me grow not only since professional point of view but above all from the human one. The university provided me with those tools that will allow me to achieve the career I have always wanted.

I would therefore like to thank all my teaching staff of the Polytechnic of Turin that they have formed my student figure. I thank my supervisor, prof. Davide Papurello, who has me followed in the drafting of this paper, and immediately proved to be extremely helpful and stimulating in carrying out this task, despite the obligatory "distance" of this period.

I want to thank my family, who allowed me to take this path, supporting me always in times of difficulty and showing great trust in me, which I hope to pay off soon. Paolo and Letizia, making you proud was my greatest motivation, which pushed me to carry out my university career in the best possible way.

I thank my friends in Italy for giving me moments of lightheartedness in the most difficult moments

Table of content

Abstract.....	5
Acknowledgments.....	7
Table of content	8
Index of figures	10
Index of tables.....	12
Chapter 1: Introduction	13
Background.....	13
Development.....	13
The Motivation for Li-ion Battery Research.....	15
Goal and Methodology	16
Chapter 2: Overview for Li-ion cell.....	17
The Structure of the Li-ion Cell.....	17
The Working Principle Lithium-ion Battery.....	20
Lithium ion charge / discharge chemistry.....	21
The Types of Lithium-ion.....	22
Lithium cobalt oxide (LiCoO ₂) – LCO	22
Lithium manganese oxide (LiMn ₂ O ₄) – LMO.....	23
Lithium Iron Phosphate(LiFePO ₄) — LFP	25
Lithium Nickel Manganese Cobalt Oxide (LiNiMnCoO ₂) — NMC	26
Lithium Nickel Cobalt Aluminum Oxide (LiNiCoAlO ₂) — NCA	28
Lithium Titanate Oxide (Li ₂ TiO ₃) — LTO	29
Types of Battery Cells	30
Cylindrical Cell.....	30
Button Cell.....	32
Prismatic cell.....	33
Pouch Cell.....	33
The Summary of the Lithium-based Batteries	36
Chapter 3: Battery Modelling	37
Introduction.....	37

Battery geometry, external and internal structures	38
Effect of temperature on the battery behaviors	38
Effect of cell design on the battery behaviors.....	39
Battery Models.....	40
Electrical-thermal modeling.....	40
Electrical Circuit Model (ECM)	41
Thermal Model.....	43
Electrochemical-thermal modelling.....	45
Chapter 4: Electrical –Thermal Model for Large Size Lithium-ion Cells	47
Thermal modelling.....	48
Model assumptions and geometry features	48
Governing equations	48
Boundary conditions	49
Heat generation measurement.....	50
Internal resistance measurement	50
Entropy coefficient measurement	54
Battery thermal model parameters	55
Chapter 5: Simulation and Results.....	58
Chapter 6: Conclusions	61
Publication bibliography	62

Index of figures

Figure 1- The Four Components of Li-ion Battery	17
Figure 2- The compound.....	18
Figure 3- The function of the electrolyte	19
Figure 4- The Discharging Process of the Lithium-ion Battery.....	20
Figure 5- The Charging Process of the Lithium-ion Battery	21
Figure 6- hex spider diagram of the LCO.....	22
Figure 7- hex spider diagram of the LMO	24
Figure 8- hex spider diagram of the LFP	25
Figure 9- hex spider diagram of the NMC.....	27
Figure 10- hex spider diagram of the NCA.....	28
Figure 11- hex spider diagram of the LTO.....	29
Figure 12- Cylindrical Cell Cross Section	31
Figure 13- The 18650 lithium-ion cell	31
Figure 14- The button cells with a cross section.....	32
Figure 15- Cross section of a prismatic cell.....	33
Figure 16- The Pouch cell.....	34
Figure 17- Swollen pouch cell.	35
Figure 18- The coupling scheme between the electrical and thermal models.....	40
Figure 19- The voltage response of a lithium-ion cell after a pulse test.	41
Figure 20- The first order Thévenin battery model.	42
Figure 21- The Electric model process.	42
Figure 22- The physics of Li-ion battery systems in different length scales.	45
Figure 23- The types of coupling between electrochemical and thermal models.	46
Figure 24- The pouch cell model with the size of the different domains.....	47
Figure 25- The pouch cell model with the size of the different domains.....	51
Figure 26- Internal resistance of charge as a function of SoC and Temperature at 0.5 It current rate.	51
Figure 27- Internal resistance of discharge as a function of SoC and Temperature at 0.5 It current rate.	52
Figure 28- Internal resistance of charge as a function of SoC and Temperature at 1 It current rate.	52
Figure 29- Internal resistance of discharge as a function of SoC and Temperature at 1 It current rate.	53
Figure 30- Internal resistance of charge as a function of SoC and Temperature at 2 It current rate.	53
Figure 31- Internal resistance of discharge as a function of SoC and Temperature at 2 It current rate.	54
Figure 32- The Cauer network.	56
Figure 33- Thermal distributions based on experimental thermal imager and modeling at 0.5 It charge current rate at 20°C of environment temperature.....	58
Figure 34- Thermal distributions based on experimental thermal imager and modeling at 0.5 It discharge current rate at 20°C of environment temperature.....	58
Figure 35- Thermal distributions based on experimental thermal imager and modeling at 1 It charge current rate at 20°C of environment temperature.....	59
Figure 36- Thermal distributions based on experimental thermal imager and modeling at 1 It discharge current rate at 20°C of environment temperature.....	59

Figure 37- Thermal distributions based on experimental thermal imager and modeling at 4 It discharge current rate at 20°C of environment temperature..... 60

Index of tables

Table 1-The characteristics of lithium cobalt oxide (LiCoO ₂).....	23
Table 2- The characteristics of lithium manganese oxide (LMO).	24
Table 3- The characteristics of lithium iron phosphate (LFP).	26
Table 4- The characteristics of lithium nickel manganese cobalt oxide (NMC).....	27
Table 5- The characteristics of lithium nickel cobalt aluminum oxide (NCA).	28
Table 6- The characteristics of lithium titanate oxide (LTO).....	30
Table 7- Summarizes the main characteristics of li-ion batteries.....	36
Table 8 - The performance parameter characteristics of cell.....	38
Table 9- The phenomena that happen when the temperature exceeds the prescribed limits.	39
Table 10- The thermal parameters used in the tab domains.	50

Chapter 1: Introduction

Background

Li-ion battery or Li-ion battery is a type of rechargeable battery. Lithium-ion batteries are commonly used for portable electronics and electric vehicles and are increasingly popular in aerospace applications. A prototype Li-ion battery was developed by Akira Yoshino in 1985, based on previous research by John Goodenough, M. Stanley Whittingham and Koichi Mizushima during the 1970s and 1980s, [1] [2] and then Development of a commercial Li-ion battery by the Sony and Asahi Kasei team led by Yoshio Nishi in 1991. [3]

Lithium batteries were suggested by British chemist M. Stanley Whittingham, who currently works at Binghamton University. Whittingham began the research that led to his progress at Stanford University. In the early 1970s, he discovered how lithium ions were stored in disulfide layers. After being hired by Exxon, he refined this innovation. Whittingham used titanium (IV) sulfide and lithium metal as electrodes. However, this rechargeable lithium battery could not become practical. Titanium disulfide was a poor choice, as it had to be manufactured under completely sealed conditions and was also very expensive (about \$ 1,000 per kilogram of titanium disulfide feedstock in the 1970s). When exposed to air, titanium disulfide reacts to form hydrogen sulfide compounds, which have an unpleasant odor and are toxic to most animals. For this reason, and other reasons, Exxon has discontinued development of a Whittingham lithium and titanium disulfide battery. Batteries with lithium metal electrodes present safety issues, as the lithium metal reacts with the water and releases flammable hydrogen gas. As a result, research has moved on to develop batteries that only contain lithium compounds, instead of metallic lithium, and that are able to accept and release lithium ions.

The lithium-ion battery (Li-ion) is an advanced battery technology that uses lithium ions as a major component in electrochemistry. During the discharge cycle, the lithium atoms in the anode ionize and are separated from their electrons. Lithium ions move from the anode and pass through the electrolyte until they reach the negative electrode, where they combine with their electrons and are electrically neutralized. Lithium ions are small enough to be able to move through a delicate permeable separation between the anode and the cathode. Partly because of the small size of lithium (only third to hydrogen and helium), Li-ion batteries are capable of very high voltage and charge storage per unit mass and unit volume. Li-ion batteries can use a number of different materials as electrodes. The most common formulations are that of lithium cobalt oxide (the cathode) and graphite (the anode), and are most common in portable electronic devices such as cell phones and laptops. Other cathode materials include lithium manganese oxide (used in electric and hybrid electric vehicles) and lithium iron phosphate. Li-ion batteries typically use ether (a class of organic compounds) as an electrolyte.

Development

- 1973 - Adam Heller proposes a lithium-thionyl chloride battery, which is still used in implanted medical devices and defense systems that require a shelf life of more than 20 years, have a high energy density, and / or withstand extreme operating temperatures. [4]

- 1977 - Samar Basu demonstrates the electrochemical intercalation of lithium in graphite at the University of Pennsylvania [5]. This led to the development of a practical lithium spliced graphite electrode at Bell Labs (LiC_6) To provide a replacement for a lithium-metal electrode battery. [6]
- 1979 - Working in separate groups, Ned A. Godshall et al., and shortly thereafter, John B. Godino (University of Oxford) and Koichi Mizushima (University of Tokyo) [7], demonstrated a rechargeable lithium cell with voltage in the 4 volt range using lithium cobalt dioxide (LiCoO_2) as the positive electrode and lithium metal as the negative electrode. This innovation provided the anode material that enabled early commercial lithium batteries. LiCoO_2 is a stable cation material that acts as a donor for lithium ions, which means that it can be used with a non-lithium cathode material.
- 1980 - Rasheed Al-Yazmi demonstrates the reverse electrochemical exchange of lithium in graphite [8] and invents the lithium graphite electrode (the anode)[9]. The available organic electrolytes at that time will be decomposed during charging with a graphite negative electrode. Yazami used a solid electrolyte to demonstrate that lithium can be reversibly cut into graphite through an electrochemical mechanism. As of 2011, Yazami's graphite electrode has been the most widely used electrode in commercial lithium-ion batteries. The cathode has its origin in PAS (a semiconducting multi-exponential material) discovered by Tokio Yamabe and later by Shjzukuni Yata in the early 1980s [10]. The seed of this technique was the discovery of conductive polymers by Professor Hideki Shirakawa and his group, and it can also be considered that it originated from the lithium-ion polacetylene battery developed by Alan McDermid and Alan J. Heiger et al. [11]
- 1982 - Godshall et al. They obtained a US patent 4,340,652 for using LiCoO_2 as a cathode in lithium batteries, based on a PhD from Stanford University at Godshall.[12]
- 1983 - Michael M Thackeray, Peter Bruce, William David and John B. Godino develop manganese spinel, Mn_2O_4 , as the charged cathode material for lithium-ion batteries. It has two flat plateaux when discharged with lithium, one at 4 volt, the stoichiometric LiMn_2O_4 , and one at 3 volt with the final stoichiometric $\text{Li}_2\text{Mn}_2\text{O}_4$. [13]
- 1985 - Akira Yoshino assembles a prototype cell using a carbon material into which lithium ions can be inserted as a single electrode, and lithium cobalt oxide (LiCoO_2) Same as the other. [14] This greatly improved safety. LiCoO_2 Enable industrial scale production and enable commercial lithium-ion battery.
- 1989 Arumugam Manthiram and John B. Goodenough discover the polyanion class of cathodes. [15] They showed that positive electrodes containing polyanions, for example, sulphates, produce higher voltages than oxides due to the inductive effect of polyyan. This class of polyanions contains substances such as lithium iron phosphate.[16]
- 1991 - Sony and Asahi Kasei release their first commercial lithium-ion battery. The Japanese team that successfully commercialized the technology, led by Yoshio Nishi.[17]
- 1996 - Goodenough, Akshaya Padhi and co-workers suggested lithium iron phosphate (LiFePO_4) and other olivine phosphates (lithium metal phosphate with the same structure of the mineral olivine) as positive electrode materials.[18]
- 1998 - CS Johnson, GT Fuji, MM Thackeray, TE Bofinger, S.A. Hackney report the discovery of high-voltage, lithium-rich NMC cathode materials.[19]
- 2001 - Arumugam Manthiram and colleagues discover that the capacity limitations of layered oxide cathodes result from chemical instability that can be understood based on the relative positions of the 3D metallic band relative to the upper part of the 2p oxygen band. This finding had significant implications for the practically accessible structural area of a Li-ion battery-layer oxide cathode, as well as its stability in terms of safety.[20]

- 2001 - Christopher Johnson, Michael Thackeray, Khalil Amin, and Jacquem Kim filed a patent for lithium-nickel-manganese-rich cobalt oxide (NMC) cathodes based on the field structure.[21]
- 2001 - Zhonghua Lu and Jeff Dahn file a patent for an NMC class of anode material, which provides improvements in safety and energy density over the widely used lithium cobalt oxide.[22]
- 2002 - Ming Chiang and his group at the Massachusetts Institute of Technology show significant improvement in the performance of lithium batteries by enhancing the conductivity of the material by doping with aluminum, niobium and zirconium. The exact mechanism that caused the increase has become the subject of widespread debate.[23]
- 2004 - Yet-Ming Chiang once again increases performance by using lithium iron phosphate particles less than 100 nm in diameter. This reduced the particle density nearly one hundred times, increased anode surface area and improved capacitance and performance. Marketing led to rapid growth of the high-capacity lithium-ion battery market, as well as a patent infringement battle between Chiang and John Goodnav.[24]
- 2005 - Y Song, PY Zavalij, and M. Stanley Whittingham report a novel cathode material consisting of two electrons of vanadium phosphate with a high energy density.[25]
- 2011 - Lithium cobalt-manganese oxide (NMC) cathodes, developed at Argonne National Laboratory, are manufactured commercially by BASF in Ohio.[26]
- 2011 - Lithium-ion batteries accounted for 66% of all portable (i.e. rechargeable) secondary battery sales in Japan.[27]
- 2012 - John Goodnav, Rashid Yazmi and Akira Yoshino receive the 2012 IEEE Medal for Environmental and Safety Technologies for developing a lithium-ion battery.[28]
- 2014 - John Godino, Yoshio Nishi, Rashid Yazami and Akira Yoshino receive the Charles Stark Draper Award from the National Academy of Engineering for their pioneering efforts in the field.[29]
- 2014 - Amprius Corp.'s commercial batteries reach 650 W / L (an increase of 20%) using silicon anode and delivered to customers.[30]
- 2016 - Koichi Mizushima and Akira Yoshino receive the NIMS Award from the National Institute of Materials Science, for Mizushima's discovery of the cathode material LiCoO_2 for a lithium-ion battery and Yoshino's development of a lithium-ion battery.[31]
- 2016 - Z. Qi and Gary Koenig report a scalable method for producing LiCoO_2 at sub-micrometer size using a model-based approach. [32]
- 2019 - Nobel Prize in Chemistry is awarded to John Godino, Stanley Whittingham and Akira Yoshino for "developing lithium ion batteries". [33]

The Motivation for Li-ion Battery Research

The interest in Li Ion cells is constantly growing due to the increase of applications that benefit from such technologies, including the automotive industry, industrial machines and energy storage. Also, Large number of automobiles are currently in use all over the world It has caused and is still causing serious problems such as air quality, global warming and Depletion of primary energy resources. Because fuel costs are rising rapidly With stringent emissions standards, it is essential to set up safe, clean and high efficient transportation. To meet the revolutionary challenge, major automotive manufacturers release the hybrid and electric vehicles onto the market. Currently lithium ion batteries are the preferred solution for hybrids and electrics Because of its high energy density and long life cycle. Specific strength is The maximum available power per unit mass, determines the battery weight of some The goal of the authority.

Specific energy is the nominal battery power per unit mass. It determines the battery weight to achieve an electric range. As shown in Fig. 1, Li-ion batteries cover a wider range of specific and energy specific energy during comparison for other types of batteries. In a hybrid electric vehicle, a battery pack is used to provide propulsion with an internal combustion engine, while in an electric vehicle, the battery pack provides all power. The battery pack is charged and discharged repeatedly during vehicle operation. This thesis will focus on characterizing the charge/discharge characteristics of Lithium ion battery materials to understand how their performance correlates with usage conditions and environmental factors. It is expected that this research will provide quantitative information on the physical and chemical properties of Lithium ion batteries, and improve our understanding on how such materials can improve the energy density, safety, and reduce costs of Lithium ion batteries.

Goal and Methodology

The goal of the thesis project is to develop a methodology for the experimental and virtual characterization of a Li-ion cell. So the first step is studying the behavior of the Li-ion cell. Then, the second step is studying the electrical model to get the required thermal parameters which will get some of it experimentally and others theoretically. In the third step the thermal parameters are used to develop the thermal model. After that, the next step is simulating the new model of Li-ion battery by using the ANSYS FLUENT to know the thermal distribution over surface of the battery and the final step is analyzing the results of the simulation.

Chapter 2: Overview for Li-ion cell

The Structure of the Li-ion Cell

Li-ion batteries are largely composed of major components: the cathode, anode, electrolyte, and separator as shown in Figure 1. A component of a Li-ion battery is no longer necessary. Every component of a Li-ion battery is essential because it cannot function when one component is missing.

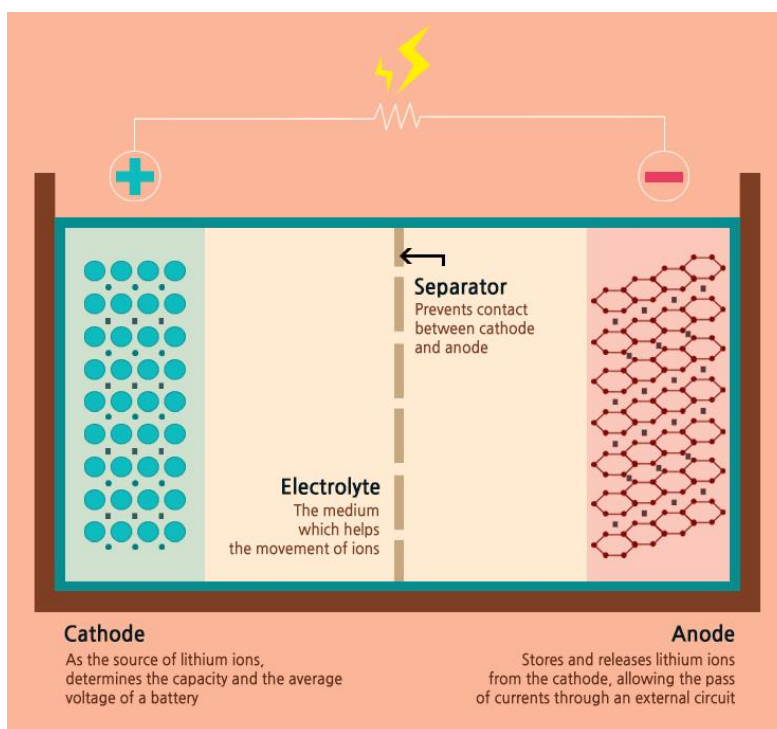


Figure 1- The Four Components of Li-ion Battery

A lithium-ion battery generates electricity through the chemical reactions of lithium, and this is the reason for the introduction of lithium into the battery and this space for lithium is called the "cathode". However, since lithium is unstable in the element form, a combine of lithium, oxygen, and lithium oxide is used for the cathode [34]. "Cathode" determines the capacity and voltage of a Li-ion battery. The material interfering with the electrode reaction of the actual battery, just like lithium oxide, is called the "active substance". In other words, in the cathode of a Li-ion battery, lithium oxide is used as the active material. If we will take a look at the cathode in Figure 2, you will find the thin aluminum foil used to hold the cathode frame covered with a compound made of active material, conductive additives and a binder. The active substance contains lithium ions, and the conductive substance is added to increase the conductivity; The binder acts as an adhesive that helps the active substance and conductive additives settle well on the aluminum substrate. The cathode plays an important role in determining the characteristics of the battery as the battery capacity and voltage are determined by the type of active material used in the cathode. The

higher the amount of lithium, the higher the capacity; The greater the potential difference between the cathode and the anode, the higher the voltage. The potential difference is small for anode depending on its type but for a cathode the potential difference is generally relatively high. As such, the cathode plays an important role in determining the battery voltage.

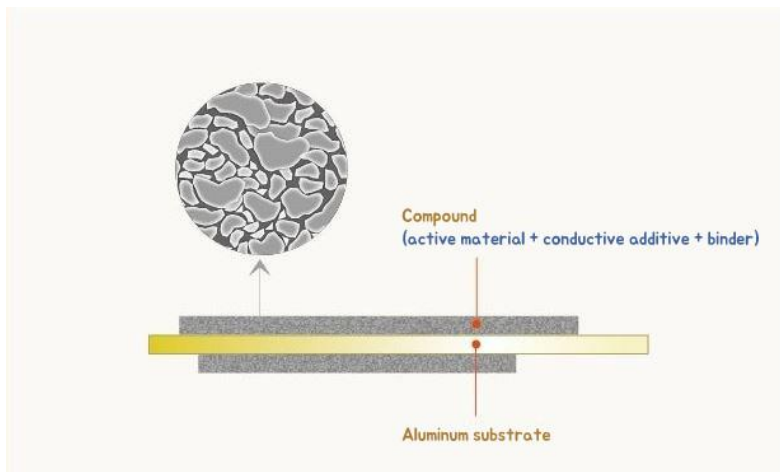


Figure 2- The compound

Just like the cathode, the anode substrate is also coated with active material. The active material of the anode plays a role in enabling electric current to flow through the external circuit while allowing absorption / emission of emitted lithium ions from the cathode. When the battery is charged, the lithium ions are stored at the anode, not the cathode. At this point, when the conducting wire connects the cathode to the anode (the discharge state), the lithium ions naturally flow to the negative electrode through the electrolyte, and the electrons (e^-) separated from the lithium ions move along the wire to generate electricity. It uses graphite anode which has stable structure, and the anode substrate is coated with active material, conductive and bonding additives. The graphite's optimum qualities such as structural stability, low electrochemical interaction, storage conditions of lots of lithium ions and price, the material is suitable for use in anode.[35]

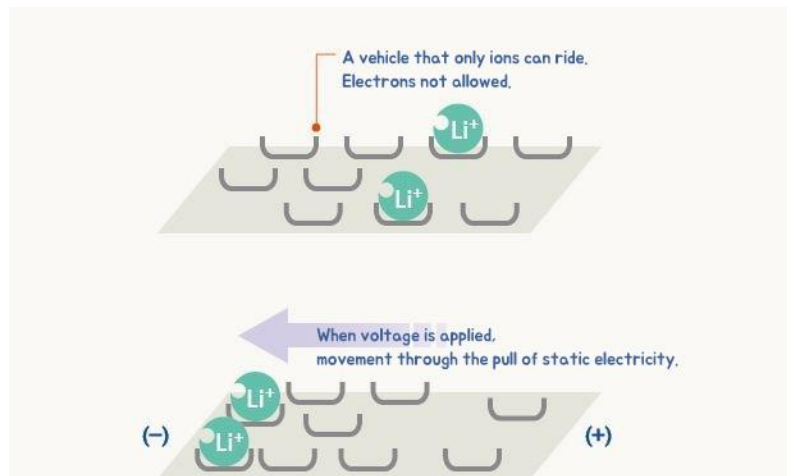


Figure 3- The function of the electrolyte

The electrolyte is the component that plays this important role. As shown in Figure 3, It serves as the medium that enables the movement of only lithium ions between the cathode and the anode (like the vehicle). When explaining the cathode and anode, it was mentioned that the lithium ions move through the electrolyte and the electrons move across the wire. This is key in enabling the battery's electricity to be used. If ions were to flow through the electrolyte, not only could we use electricity, but safety would be compromised. For the electrolyte, materials with high ionic conductivity are mainly used so that lithium ions move back and forth easily. The electrolyte consists of salts, solvents, and additives. Salts are the pathway for the movement of lithium ions, and solvents are organic fluids used to dissolve salts. Additives are added in small quantities for specific purposes. The electrolyte created in this way only allows ions to move to the electrodes and does not allow electrons to pass through. Additionally, the velocity of lithium ion movement depends on the type of electrolyte. Thus, only electrolytes that meet strict conditions can be used.

While the cathode and anode determine the basic performance of a battery, the electrolyte and separator determine the integrity of the battery. The separator acts as a physical barrier separating the cathode and the anode. It prevents direct flow of electrons and only allows ions to pass through the internal microscopic hole. Therefore, it must meet all physical and electrochemical conditions. The commercial separators we have today are synthetic resins such as polyethylene (PE) and polypropylene (PP).

So far, we have looked at the four main components that determine the performance of Li-ion batteries. Currently, The companies are promoting the research and development of new materials to improve battery performance by innovation of high-capacity or high-efficiency lithium-ion battery.

The Working Principle Lithium-ion Battery

When the lithium-ion battery discharges, as shown in Figure 4 positively charged lithium ions (Li^+) move from the negative anode to the positive cathode. They do this by moving through the electrolyte until they reach the positive electrode. There, they are deposited. The electrons, on the other hand, move from the anode to the cathode.

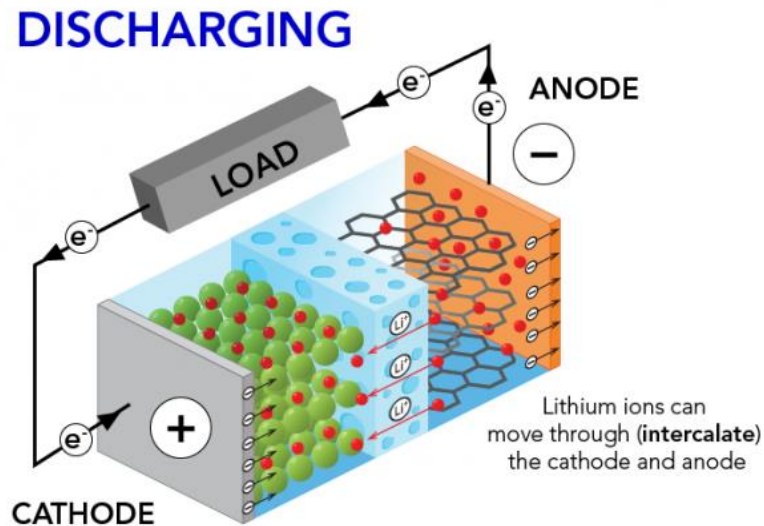


Figure 4- The Discharging Process of the Lithium-ion Battery

When you charge a lithium-ion battery, as shown in Figure 5 the exact opposite process happens. The lithium ions move back from the cathode to the anode. The electrons move from the anode to the cathode. As long as lithium ions are making the trek from one electrode to another, there is a constant flow of electrons. This provides the energy to keep your device running. Since this cycle can be repeated hundreds of times [36], this type of battery is rechargeable.

CHARGING

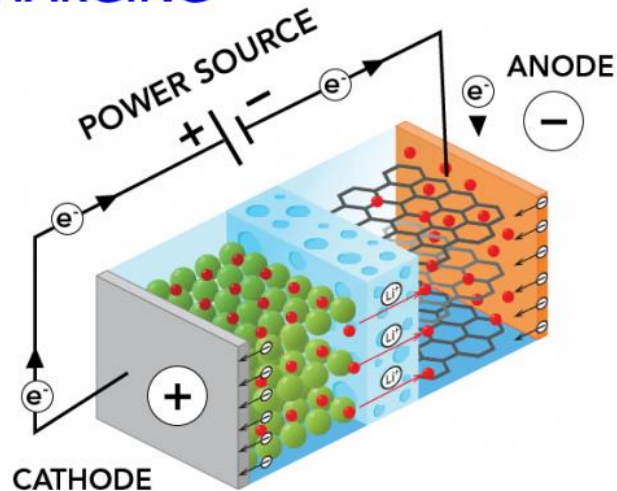
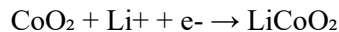


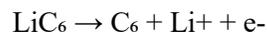
Figure 5- The Charging Process of the Lithium-ion Battery

Lithium ion charge / discharge chemistry

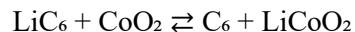
In very basic terms, the charge and discharge of a lithium ion battery is relatively easy to explain. When the lithium ion cell or battery is discharging it provides current to an external circuit. Internally the anode releases lithium ions in an oxidation process which pass to the cathode. The electrons from the ions that have been created flow in the opposite direction, flowing out into the electrical or electronic circuit that is being powered. The ions and electrons then reform at the cathode. This process releases the chemical energy that is stored in the cell in the form of electrical energy. So in the discharging, the Reduction takes place at the cathode. There, cobalt oxide combines with lithium ions to form lithium-cobalt oxide (LiCoO_2). The half-reaction is:



Oxidation takes place at the anode. There, the graphite intercalation compound LiC_6 forms graphite (C_6) and lithium ions. The half-reaction is:



During the charging cycle, the reactions occur in the reverse direction with lithium ions passing from the cathode through the electrolyte to the anode. The electrons provided by the external circuit then combine with the lithium ions to provide the stored electrical energy. So we can say that the full reaction (left to right = discharging, right to left = charging):



It should be remembered that the charging process is not totally efficient - some energy is lost as heat, although efficiency levels of around 95% or a little less are typical.

The Types of Lithium-ion

Lithium ion is named for its active substances; The words are either completely written or abbreviated with their chemical symbols. A series of letters and numbers grouped together can be difficult to remember and even difficult to pronounce, as battery chemistry is defined by abbreviated letters. For example, lithium cobalt oxide, which is one of the most common lithium ions, contains the chemical codes (LiCoO₂), the abbreviation LCO. For reasons of simplicity, the Li-cobalt short form can also be used for this battery [37]. Cobalt is the main active substance that gives this battery its characteristic. Other Li-ion chemistries are given similar short names. There are six of the most common lithium ions. Lithium-ion batteries can be designed to have optimum capacity with the disadvantage of limited load, slow charging, and reduced life. An industrial battery may have a moderate Ah rating but the focus is on durability. Specific power supplies only part of battery performance.

Lithium cobalt oxide (LiCoO₂) – LCO

LCO is a popular choice for cell phones, laptops, and digital cameras because it has a high specific energy. The battery is made of cobalt oxide cathode and graphite carbon anode [38]. The cathode has a layered structure, and during the discharge, the lithium ions move from the positive electrode to the negative electrode. The flow reverses on charge. The disadvantage of Li-cobalt is relatively short life, low thermal stability, and limited loading capabilities (specific power). Like other cobalt-blended Li-ion, Li-cobalt has a graphite anode that limits the cycle life through a variable solid electrolyte interface (SEI), thickens on the anode and coating the lithium during fast charging and charging at low temperature. Newer systems incorporate nickel, manganese and / or aluminum to improve longevity, loading capabilities, and cost. Li-cobalt should not be charged and discharged at a current higher than its C rating. This means that 18650 cells with 2,400 mAh can only be charged and discharged at 2,400 mA. Forcing a fast charge or a load load higher than 2,400 mAh causes overheating and undue stress. For the best fast charging, the manufacturer recommends a C-rating of 0.8 ° C, or about 2000 mA. (See BU-402: What is the C rate). Mandatory battery protection circuit limits the rate of charge and discharge to a safe level of about 1 ° C for the power cell.

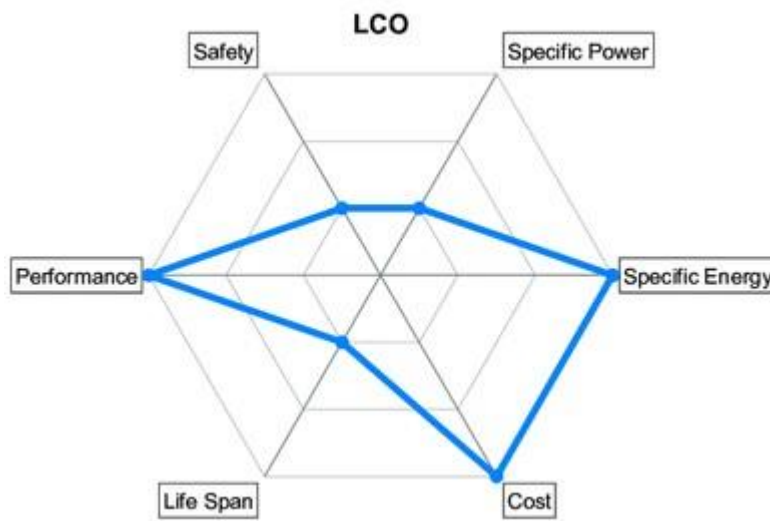


Figure 6- hex spider diagram of the LCO

The hex spider diagram as shown in Figure 6 that summarizes the Li-cobalt performance in terms of specific power or capacitance related to uptime; Specific power or the ability to deliver a high current; safety; Performance in hot and cold temperatures; The life span reflects the life cycle and longevity; And cost. Other important characteristics that do not appear in spider webs are toxicity, fast charging and self-discharging capabilities, and shelf life. Also Table 1 is showing the Characteristics of lithium cobalt oxide.

Voltages	3.60V nominal; typical operating range 3.0–4.2V/cell
Specific energy (capacity)	150–200Wh/kg. Specialty cells provide up to 240Wh/kg.
Charge (C-rate)	0.7–1C, charges to 4.20V (most cells); 3h charge typical. Charge current above 1C shortens battery life.
Discharge (C-rate)	1C; 2.50V cut off. Discharge current above 1C shortens battery life.
Cycle life	500–1000, related to depth of discharge, load, temperature
Thermal runaway	150°C (302°F). Full charge promotes thermal runaway
Applications	Mobile phones, tablets, laptops, cameras
Comments	Very high specific energy, limited specific power. Cobalt is expensive. Serves as Energy Cell. Market share has stabilized.

Table 1-The characteristics of lithium cobalt oxide (LiCoO₂).

Lithium manganese oxide (LiMn₂O₄) – LMO

The architecture forms a three-dimensional spinel structure that improves the flow of ions on the electrode, resulting in less internal resistance and better handling of current. Another advantage of the spinel is higher thermal stability and enhanced safety, but the life cycle and calendar life are limited. The low internal resistance of the cell enables fast charging and high current discharging. In 18650 packaging, Li-manganese can be discharged into 20-30A streams with moderate heat build-up. It is also possible to apply load pulses of 1 second up to 50 amps. Continuous high load in this current may cause heat build-up and the cell temperature cannot exceed 80 ° C (176 ° F). Li-manganese is used in electric and medical instruments as well as hybrid and electric vehicles.

Li-manganese has a capacity that is roughly one-third lower than Li-cobalt. Design flexibility allows engineers to maximize the battery for either optimal longevity (life span), maximum load current (specific power) or high capacity (specific energy). For example, the long-life version in the 18650 cell has a moderate capacity of only 1,100mAh; the high-capacity version is 1,500mAh.

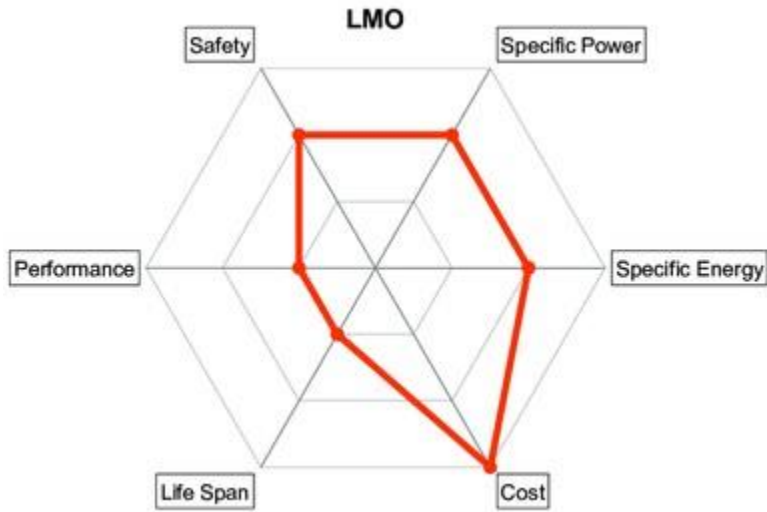


Figure 7- hex spider diagram of the LMO

The hex spider diagram as shown in Figure 7 that summarizes the typical Li-manganese battery. The characteristics appear marginal but newer designs have improved in terms of specific power, safety and life span. Pure Li-manganese batteries are no longer common today; they may only be used for special applications. Also Table 2 is showing the Characteristics of Lithium Manganese Oxide.

Voltages	3.70V (3.80V) nominal; typical operating range 3.0–4.2V/cell
Specific energy (capacity)	100–150Wh/kg
Charge (C-rate)	0.7–1C typical, 3C maximum, charges to 4.20V (most cells)
Discharge (C-rate)	1C; 10C possible with some cells, 30C pulse (5s), 2.50V cut-off
Cycle life	300–700 (related to depth of discharge, temperature)
Thermal runaway	250°C (482°F) typical. High charge promotes thermal runaway
Applications	Power tools, medical devices, electric powertrains
Comments	High power but less capacity; safer than Li-cobalt; commonly mixed with NMC to improve performance.

Table 2- The characteristics of lithium manganese oxide (LMO).

Most Li-manganese batteries are blended with lithium-nickel-manganese cobalt oxide (NMC) to improve specific power and extend life. This combination brings out the best in every system, and the LMO (NMC) is chosen for most electric vehicles, such as the Nissan Leaf, Chevy Volt, and BMW i3. The LMO portion of the battery, which can be around 30 percent, provides a high current boost on acceleration; The NMC segment gives a long driving range.

Li-ion research is strongly attracted towards combining Li-manganese with cobalt, nickel, manganese, and / or aluminum as active cathode materials. In some architectures, a small amount of silicon is added to the anode. This provides a capacity increase of 25 percent; However, the gain is usually associated

with a shorter life cycle as the silicone grows and contracts with charge and discharge, causing mechanical stress.

Lithium Iron Phosphate(LiFePO₄) — LFP

Li-phosphate provides good electrochemical performance with low resistance. This is made possible with a phosphate nanocathode material. The main benefits are high current rating and long cycle life, along with good thermal stability, enhanced safety and tolerance in case of abuse.

Li-phosphate is more durable to fully charged conditions and is less stressful than other lithium ion systems if kept at high voltage for a long time. As a trade off, its low nominal voltage of 3.2 V / cell reduces the specific energy less than that of lithium-ion mixed with cobalt. With most batteries, cold temperature reduces performance and higher storage temperature reduces service life, and Li-phosphate is no exception. Li-phosphate has a higher self-discharge than other Li-ion batteries, which can cause balance problems with aging. This can be mitigated by purchasing high-quality cells and / or using sophisticated control electronics, both of which increase the cost of the package. Cleanliness in manufacturing is important to longevity. There is no possibility of moisture, lest the battery provide only 50 cycles.

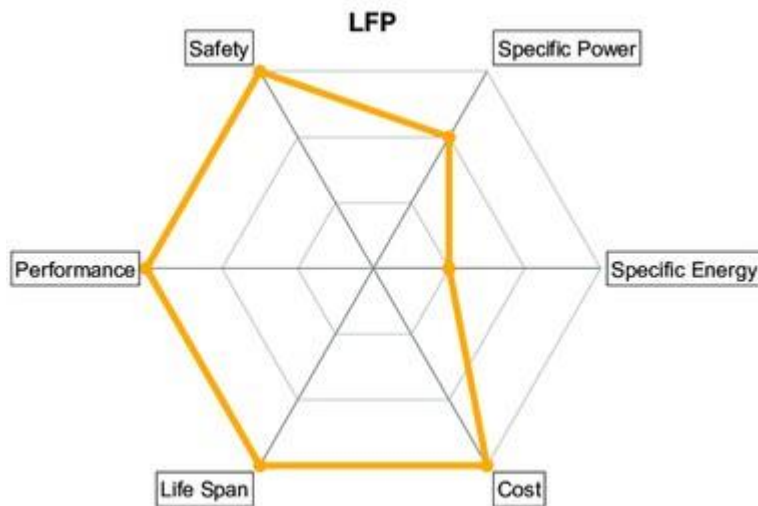


Figure 8- hex spider diagram of the LFP

The hex spider diagram as shown in Figure 8 that summarizes the typical Li-phosphate battery. The characteristics appear that Li-phosphate has excellent safety and long life span but moderate specific energy and elevated self-discharge. Also Table 3 is showing the Characteristics of Lithium Iron Phosphate.

Voltages	3.20, 3.30V nominal; typical operating range 2.5–3.65V/cell
Specific energy (capacity)	90–120Wh/kg
Charge (C-rate)	1C typical, charges to 3.65V; 3h charge time typical
Discharge (C-rate)	1C, 25C on some cells; 40A pulse (2s); 2.50V cut-off (lower than 2V causes damage)
Cycle life	2000 and higher (related to depth of discharge, temperature)
Thermal runaway	270°C (518°F) Very safe battery even if fully charged
Cost	~\$580 per kWh (Source: RWTH, Aachen)
Applications	Portable and stationary needing high load currents and endurance
Comments	Very flat voltage discharge curve but low capacity. One of safest Li-ions. Used for special markets. Elevated self-discharge.

Table 3- The characteristics of lithium iron phosphate (LFP).

Li-phosphate is often used to replace the lead acid starter battery. Four cells in series produce 12.80 volts, which is a voltage similar to six 2 volt lead acid cells in the series. The compounds charge lead acid to 14.40 volts (2.40 volts / cell) and maintain a higher charge. A higher charge is applied to maintain a full charge and prevent sulfates on lead acid batteries. Li-phosphate is tolerant of some overcharges; However, maintaining the voltage at 14.40 volts for an extended period, as most vehicles do on a long road trip, can stress lithium phosphate. Time will determine how long the Li-Phosphate lasts as a replacement for lead acid with a regular vehicle charging system. The cold temperature also reduces the performance of Li-ion and this may affect its recycling ability in extreme cases.

Lithium Nickel Manganese Cobalt Oxide (LiNiMnCoO₂) — NMC

One of the most successful Li-ion systems is the cathode mixture of nickel, manganese and cobalt (NMC). Similar to Li-manganese, these systems can be designed to act as power cells or power cells. For example, the NMC capacity of the 18650 cell for the moderate load condition is around 2800mAh and it can deliver 4A to 5A; The capacity of NMC in the same cell optimized for a given power is around 2000mAh but provides a continuous discharge current of 20A. Silicon based anode will go 4000mAh and higher but with lower load capacity and shorter cycle life. Silicon added to graphite has the disadvantage that the anode grows and contracts with charging and discharging, making the cell mechanically unstable.

The secret of NMC is its combination of nickel and manganese. An example of this is table salt where the main ingredients, sodium and chloride, are toxic on their own but mixing them acts as a seasoning salt and a food preservative. Nickel is known for its high specific energy but poor stability; manganese has the benefit of forming a spinel structure to achieve low internal resistance but offers a low specific energy. Combining the metals enhances each other strengths.

NMC is the battery of choice for electric gadgets, e-bikes, and other electric powertrains. Typically, the cathode composition is one-third of nickel, one-third of manganese, and one-third of cobalt, also known

as 1-1-1. Cobalt is expensive and limited in supply. Battery manufacturers are reducing the cobalt content with some performance compromises.

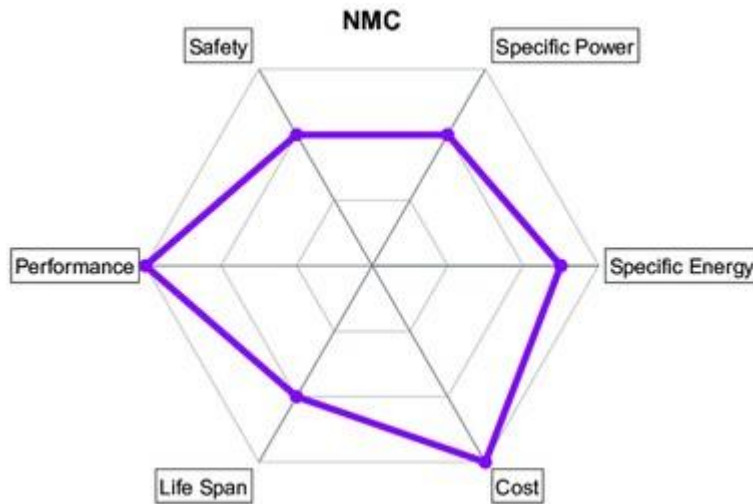


Figure 9- hex spider diagram of the NMC

The hex spider diagram as shown in Figure 9 that summarizes the typical Li-phosphate battery. The characteristics appear that NMC has good overall performance and excels on specific energy. This battery is the preferred candidate for the electric vehicle and has the lowest self-heating rate. Also Table 4 is showing the Characteristics of Lithium Nickel Manganese Cobalt Oxide.

Voltages	3.60V, 3.70V nominal; typical operating range 3.0–4.2V/cell, or higher
Specific energy (capacity)	150–220Wh/kg
Charge (C-rate)	0.7–1C, charges to 4.20V, some go to 4.30V; 3h charge typical. Charge current above 1C shortens battery life.
Discharge (C-rate)	1C; 2C possible on some cells; 2.50V cut-off
Cycle life	1000–2000 (related to depth of discharge, temperature)
Thermal runaway	210°C (410°F) typical. High charge promotes thermal runaway
Cost	~\$420 per kWh (Source: RWTH, Aachen)
Applications	E-bikes, medical devices, EVs, industrial
Comments	Provides high capacity and high power. Serves as Hybrid Cell. Favorite chemistry for many uses; market share is increasing.

Table 4- The characteristics of lithium nickel manganese cobalt oxide (NMC).

There is a move towards NMC-blended Li-ion as the system can be built economically and it achieves a good performance. The three active materials of nickel, manganese and cobalt can easily be blended to suit a wide range of applications for automotive and energy storage systems (ESS) that need frequent cycling. The NMC family is growing in its diversity

Lithium Nickel Cobalt Aluminum Oxide (LiNiCoAlO₂) — NCA

NCA, is a li-ion battery type that is rarely seen in consumer applications but is being investigated for the automotive industry. NCA shares similarities with NMC by offering high specific energy, reasonably good specific power and a long life span but the negatives are High cost and marginal safety. NCA is a further development of lithium nickel oxide; adding aluminum gives the chemistry greater stability. The hex spider diagram as shown in Figure 10 that summarizes the typical Li- Nickel Cobalt Aluminum Oxide battery. Also Table 5 is showing the Characteristics of Lithium Nickel Cobalt Aluminum Oxide.

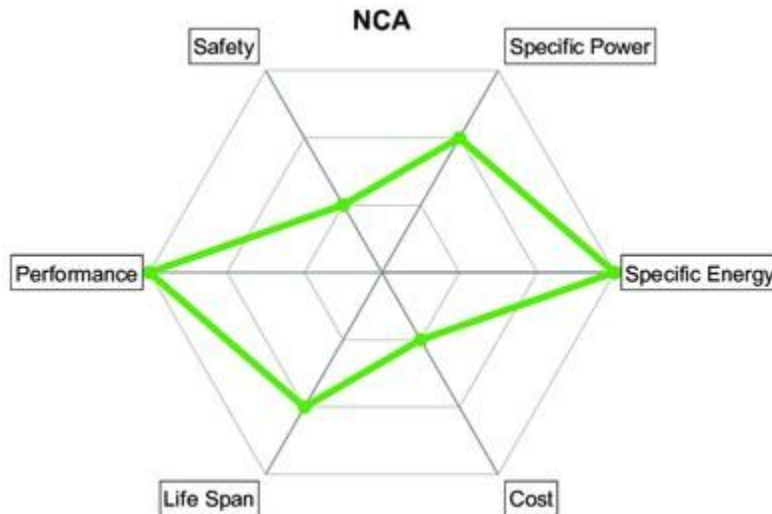


Figure 10- hex spider diagram of the NCA

Voltages	3.60V nominal; typical operating range 3.0–4.2V/cell
Specific energy (capacity)	200-260Wh/kg; 300Wh/kg predictable
Charge (C-rate)	0.7C, charges to 4.20V (most cells), 3h charge typical, fast charge possible with some cells
Discharge (C-rate)	1C typical; 3.00V cut-off; high discharge rate shortens battery life
Cycle life	500 (related to depth of discharge, temperature)
Thermal runaway	150°C (302°F) typical, High charge promotes thermal runaway
Cost	~\$350 per kWh (Source: RWTH, Aachen)
Applications	Medical devices, industrial, electric powertrain (Tesla)
Comments	Shares similarities with Li-cobalt. Serves as Energy Cell.

Table 5- The characteristics of lithium nickel cobalt aluminum oxide (NCA).

Lithium Titanate Oxide (Li_2TiO_3) — LTO

LTO replaces the graphite contained in the anode of a typical lithium-ion battery and the material forms in the structure of a spinel. The cathode can be lithium manganese oxide or NMC. LTO has a nominal cell voltage of 2.40V, can be charged quickly and provides a high discharge current of 10 ° C, or 10 times the rated capacity. The cycle count is said to be higher than that of a regular Li-ion. LTO is safe, has excellent low-temperature discharge characteristics and obtains a capacity of 80 percent at -30°C (-22°F).

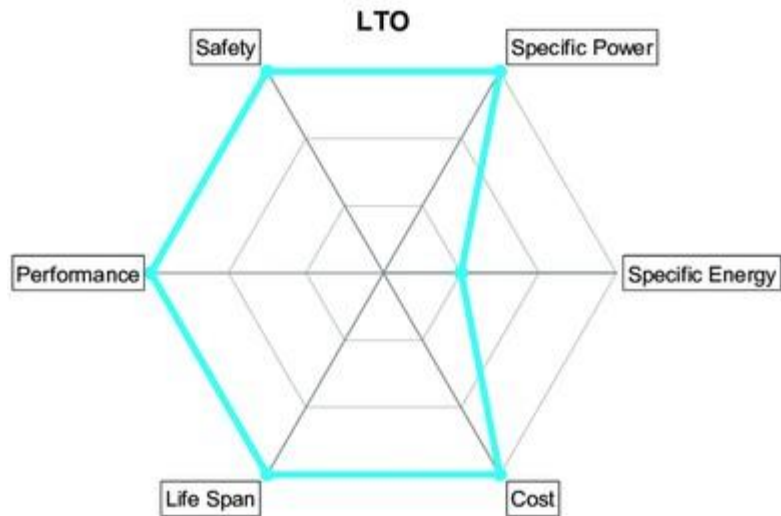


Figure 11- hex spider diagram of the LTO

LTO (usually $\text{Li}_4\text{Ti}_5\text{O}_{12}$) has advantages over traditional cobalt-mixed Li-ion with graphite anode by achieving the property of non-stress, no SEI film formation and no lithium coating when fast charging and charging at low temperature. Thermal stability under high temperature is also better than other Li-ion systems; However, the battery is quite expensive. At only 65Wh / kg, the specific energy is low, rivaling that of NiCd. LTO charges to 2.80V / cell, and discharge end is 1.80V / cell. Figure 11 shows the characteristics of Lithium Titanate that excels in safety, low-temperature performance and life span. Efforts are being made to improve the specific energy and lower cost. Also Table 6 is showing the Characteristics of Lithium Titanate (LTO). Typical uses are electric powertrains, solar powered UPS and street lighting.

Voltages	2.40V nominal; typical operating range 1.8–2.85V/cell
Specific energy (capacity)	50–80Wh/kg
Charge (C-rate)	1C typical; 5C maximum, charges to 2.85V
Discharge (C-rate)	10C possible, 30C 5s pulse; 1.80V cut-off on LCO/LTO
Cycle life	3,000–7,000
Thermal runaway	One of safest Li-ion batteries
Cost	~\$1,005 per kWh (Source: RWTH, Aachen)
Applications	UPS, electric powertrain (Mitsubishi i-MiEV, Honda Fit EV), solar-powered street lighting
Comments	Long life, fast charge, wide temperature range but low specific energy and expensive. Among safest Li-ion batteries.

Table 6- The characteristics of lithium titanate oxide (LTO).

Types of Battery Cells

At present, there are three main types of mainstream lithium battery structures, namely, cylindrical, prismatic and pouch cells. Different lithium battery structure means different characteristics, and each has its own advantages and disadvantages.

Cylindrical Cell

The cylindrical cell remains one of the most widely used packaging styles for primary and secondary batteries. The advantages are ease of manufacture and good mechanical stability. The tubular cylinder can bear high internal pressures without deformation. Many lithium-nickel-based cylindrical cells include a positive temperature coefficient (PTC) switch [38]. When exposed to excessive current, the conductive polymer usually heats up and becomes resistive, which stops the current flow and acts as a short-circuit protection. Once the short is removed, the PTC cools down and returns to the conductive state. Most cylindrical cells also have a decompression mechanism, and the simpler design uses a membrane seal that ruptures under high pressure. Leakage and dryness may occur after the membrane is broken. Resealable openings with a spring-loaded valve are the preferred design. Some consumer Li-ion cells include a charge interrupt device (CID) that physically and irreversibly separates the cell when activated for an unsafe pressure build-up. Figure 12 shows a cylindrical cell cross section.

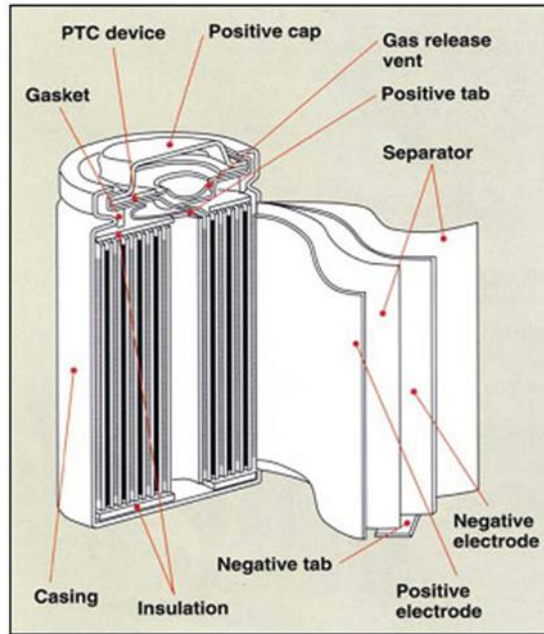


Figure 12- Cylindrical Cell Cross Section

The cylindrical cell design has good cycling ability, provides long straightening life and is economical, but it is heavy and low packing density due to the cavities of space. Typical applications of the cylindrical cell are power tools, medical instruments, laptops, and e-bikes. To allow for differences within a specific size, manufacturers use partial cell lengths, such as the half and three-quarter formats, and nickel-cadmium provides the widest variety of cell options. Some of them extended to nickel-metal hydride, but not to the lithium ion because this chemistry established their own forms. The Model 18650 shown in Figure 13 The Model 18650 remains one of the most popular cell bundles. Typical applications for the 18650 Li-ion are electrical instruments, medical devices, laptops, and e-bikes. The metallic cylinder measure 18mm in diameter and 65mm the length. The larger 26650 cell measures 26mm in diameter.



Figure 13- The 18650 lithium-ion cell

The larger 26650 cell with a diameter of 26mm does not enjoy the same popularity as the 18650. The 26650 is commonly used in load-leveling systems. A thicker cell is said to be harder to build than a thinner one. Making the cell longer is preferred. There is also a 26700 made by E-One Moli Energy.

Even though the cylindrical cell does not fully utilize the space by creating air cavities on side-by-side placement, the 18650 has a higher energy density than a prismatic/pouch Li-ion cell. The 3Ah 18650 delivers 248Ah/kg, whereas a modern pouch cell has about 140Ah/kg. The higher energy density of the cylindrical cell compensates for its less ideal stacking abilities and the empty space can always be used for cooling to improve thermal management.

Cell disintegration cannot always be prevented but propagation can. Cylindrical cells are often spaced apart to stop propagation should one cell take off. Spacing also helps in the thermal management. In addition, a cylindrical design does not change size. In comparison, a 5mm prismatic cell can expand to 8mm with use and allowances must be made.

Button Cell

The button cell, also known as the coin cell, enabled a compact design in mobile devices of the 1980s. A higher voltage was achieved by stacking cells in a tube. Cordless phones, medical devices, and airport security sticks used these batteries. Although small and inexpensive to build, the stacked button cell is no longer preferred and has given way to more conventional battery formats. The button cell defect enlarges if it is charged too quickly. Button cells do not have safety vent and can only be charged 10-16 hours; However, the newer designs claim fast charging capability. However most of the button cells in use today are non-rechargeable and are found in medical implants, watches, hearing aids, car keys and memory backup. The Button cells provides small size, most are primary for single-cell use. Figure 14 illustrates the button cells with a cross section.

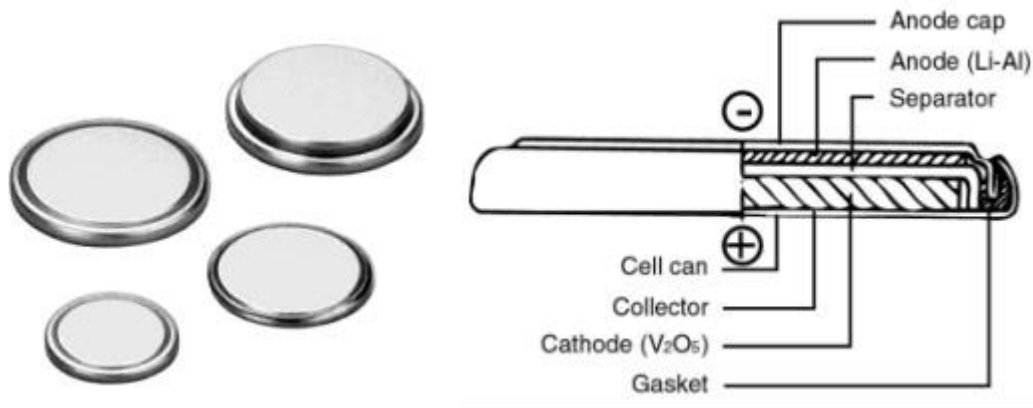


Figure 14- The button cells with a cross section.

Prismatic cell

The modern prismatic cell meets the demand for thin sizes. Wrapped in elegant packaging that resembles a box of chewing gum or a small chocolate bar, the prismatic cells make optimal use of the space using a layered approach. Other designs are rolled up and flattened into a prismatic pseudo-gel roll. These cells are mostly found in cell phones, tablets, and low-end laptops ranging from 800 mAh to 4000 mAh[39]. There is no universal format and every manufacturer designs it themselves. Prismatic cells are also available in large formats. Packaged in welded aluminum cans, the cells provide capacities from 20 to 50 Ah and are primarily used in electric powertrains in hybrid and electric vehicles. The prismatic cell improves space utilization and allows flexible design but it can be more expensive to manufacture, less efficient in thermal management and have a shorter cycle life than the cylindrical design. Allow for some swelling. Figure 15 shows the prismatic cell.

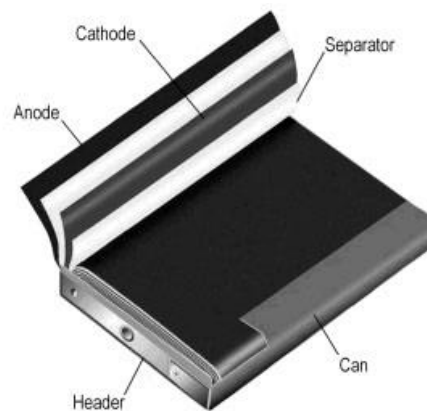


Figure 15- Cross section of a prismatic cell.

The prismatic cell requires a firm enclosure to achieve compression. Some swelling due to gas buildup is normal, and growth allowance must be made; a 5mm (0.2”) cell can grow to 8mm (0.3”) after 500 cycles. Discontinue using the battery if the distortion presses against the battery compartment. Bulging batteries can damage equipment and compromise safety.

Pouch Cell

In 1995, the bag cell surprised the battery scientist with a radical new design. Instead of using a metal cylinder and a glass-to-metal electrode, the conductive electrodes were welded and brought outward in a completely sealed manner. Figure 16 shows the pouch cell.



Figure 16- The Pouch cell.

The pouch cell provides a simple, flexible and lightweight solution to battery design. Some stack pressure is recommended but swelling should be allowed. Bag cells can provide high load currents but perform better under light loading and moderate charging conditions.

The case cell achieves optimum space utilization and achieves 90-95 percent packing efficiency, the highest among battery packs. Ditching the metal case reduces weight, but the cell needs a support and allowance to expand the battery compartment. The bag packaging is used in consumer, military, and automotive applications. There are no standard cyst cells; Each manufacturer designs himself. The packaging for the bags is usually the Li-polymer type. Small cells are popular for portable applications that require high load currents, such as drones and hobby gadgets. Larger cells operate in the 40Ah range in Energy Storage Systems (ESS) because fewer cells simplify battery design.

Although easily stacked, swelling should be provided. While small cyst packages can grow 8-10 percent over 500 cycles, large cells may expand to this size in 5,000 cycles. It is best not to stack the cells of the bag on top of one another but to place them flat side by side or allow extra space between them. Avoid sharp edges that could squeeze the cells of the bag as it expands. Extreme swelling is a concern. Users of bag packaging have reported swelling of as much as 3 percent when running a bad batch. The resulting stress can break the battery cover and, in some cases, break the screen and electronic circuit boards. Stop using an inflated battery and do not puncture the inflation cell too close to heat or fire. Leaked gases can ignite. Figure 17 shows a swollen pouch cell.



Figure 17- Swollen pouch cell.

Swelling can occur due to gassing. Improvements are being made with newer designs. Large pouch cells designs experience less swelling. The gases contain mainly CO₂ (carbon dioxide) and CO (carbon monoxide).

Pouch cells are manufactured by adding a temporary “gasbag” on the side. Gases escape into the gasbag while forming the solid electrolyte interface (SEI) during the first charge. The gasbag is cut off and the pack is resealed as part of the finishing process. Forming a solid SEI is key to good formatting practices. Subsequent charges should produce minimal gases, however, gas generation, also known as gassing, cannot be fully avoided. It is caused by electrolyte decomposition as part of usage and aging. Stresses, such as overcharging and overheating promote gassing. Ballooning with normal use often hints to a flawed batch.

The technology has matured and prismatic and pouch cells have the potential for greater capacity than the cylindrical format. Large flat packs serve electric powertrains and Energy Storage System (ESS) with good results. The cost per kWh in the prismatic/pouch cell is still higher than with the 18650 cell but this is changing.

The Summary of the Lithium-based Batteries

The term lithium ion refers to a family of batteries that share similarities, but the chemistry can vary greatly. Li-cobalt, Li-manganese, NMC, and Li-aluminum are similar in that they provide high capacity and are used in portable applications. Li-phosphate and Li-titanate have lower voltage and lower capacity, but are very durable. These batteries are mainly found in both wheeled and stationary applications. Table 7 summarizes the main characteristics of Li-ion batteries[40].

Chemistry	Lithium Cobalt Oxide	Lithium Manganese Oxide	Lithium Nickel Manganese Oxide	Lithium Iron Phosphate	Lithium Nickel Cobalt Aluminum Oxide	Lithium Titanate Oxide
Short form	Li-cobalt	Li-manganese	NMC	Li-phosphate	Li-aluminum	Li-titanate
Abbreviation	LiCoO ₂ (LCO)	LiMn ₂ O ₄ (LMO)	LiNiMnCoO ₂ (NMC)	LiFePO ₄ (LFP)	LiNiCoAlO ₂ (NCA)	Li ₂ TiO ₃ (common) (LTO)
Nominal voltage	3.60V	3.70V (3.80V)	3.60V (3.70V)	3.20, 3.30V	3.60V	2.40V
Full charge	4.20V	4.20V	4.20V (or higher)	3.65V	4.20V	2.85V
Full discharge	3.00V	3.00V	3.00V	2.50V	3.00V	1.80V
Minimal voltage	2.50V	2.50V	2.50V	2.00V	2.50V	1.50V (est.)
Specific Energy	150–200Wh/kg	100–150Wh/kg	150–220Wh/kg	90–120Wh/kg	200–260Wh/kg	70–80Wh/kg
Charge rate	0.7–1C (3h)	0.7–1C (3h)	0.7–1C (3h)	1C (3h)	1C	1C (5C max)
Discharge rate	1C (1h)	1C, 10C possible	1–2C	1C (25C pulse)	1C	10C possible
Cycle life (ideal)	500–1000	300–700	1000–2000	1000–2000	500	3,000–7,000
Thermal runaway	150°C (higher when empty)	250°C (higher when empty)	210°C (higher when empty)	270°C (safe at full charge)	150°C (higher when empty)	One of safest Li-ion batteries
Maintenance	Keep cool; store partially charged; prevent full charge cycles, use moderate charge and discharge currents					
Packaging (typical)	18650, prismatic and pouch cell	prismatic	18650, prismatic and pouch cell	26650, prismatic	18650	prismatic
History	1991 (Sony)	1996	2008	1996	1999	2008
Applications	Mobile phones, tablets, laptops, cameras	Power tools, medical devices, powertrains	E-bikes, medical devices, EVs, industrial	Stationary with high currents and endurance	Medical, industrial, EV (Tesla)	UPS, EV, solar street lighting
Comments	High energy, limited power. Market share has stabilized.	High power, less capacity; safer than Li-cobalt; often mixed with NMC to improve performance.	High capacity and high power. Market share is increasing. Also NCM, CMN, MNC, MCN	Flat discharge voltage, high power low capacity, very safe; elevated self-discharge.	Highest capacity with moderate power. Similar to Li-cobalt.	Long life, fast charge, wide temperature range and safe. Low capacity, expensive.

Table 7- Summarizes the main characteristics of li-ion batteries.

Chapter 3: Battery Modelling

Introduction

In this chapter, we will develop a two-dimensional thermos-electric model in order to examine and analyze the temperature distribution on the battery surface. we will use the ANSYS software to simulate the model development. Moreover, we will define the proposed thermal model parameters. Also, we will investigate the thermal behavior of the battery under different environmental conditions as well as during conditions of misuse.

Lithium-ion batteries emerged as the main energy storage technology and are now the main technology for portable devices. Due to its high capabilities, high energy density, high power, as well as good life, it is now the preferred battery technology, which has been able to provide longer driving range and acceleration suitable for electric drive vehicles such as Hybrid Electric Vehicles (HEVs), Battery Electric Vehicles (BEVs) and Hybrid Electric Vehicles (PHEVs) [41], [42] - [43]. However, cost, security and temperature issues remain obstacles to its wide application. As is known, during the process of discharging or charging, various exothermic chemical and electrochemical reactions occur. These phenomena generate heat that accumulates inside the battery and thus speeds up the interaction between the components of the cell. As current discharging/charging rates rise, the heat generation in the battery increases exponentially. If the heat transfer from the battery to the surroundings is insufficient, the battery can overheat very quickly and exceed the safe temperature range. For optimum performance, safety and durability considerations, the battery must operate within the safe operating range of voltage, current, and temperature as specified by the battery manufacturer. The voltage range is between maximum voltage (3.65V) and minimum voltage (2V), the temperature range depends on the operating mode (charging and discharging) and varies between [-20 °C; 60 °C] and [0 °C; 40 °C] during discharging and charging, respectively. These ranges can change according to the cell chemistry and battery manufacturer [44]. On the issue of temperature, a Thermal Battery Management System (BTMS) is needed as part of the entire battery system to implement to keep the batteries operating temperature between those limits. BTMS must be optimized to suit the specific operational conditions of each application. A better understanding, evaluation, and comparison of different BTMS in an objective way is needed for optimal battery performance. This would also give the opportunity to make BTMS smaller, cheaper, compact, efficient and light, and customized for its own area of operation. If less attention was spent on BTMS, issues could arise about safety, durability, life cycle and range.

In this way, designing, evaluating and comparing BTMS is critical to improving battery performance and setting future targets for projecting BEVs. This chapter first focuses on giving a brief description of the effect of temperature on a lithium-ion battery cell. Then review the different thermal models of batteries that have been developed and analyze their characteristics. Furthermore, the various battery thermal management systems found in the literature have also been discussed in depth. Some basic numerical methods and software tools are also analyzed and documented.

Choice of the battery chemistry in this thesis, it will be the lithium iron phosphate battery (EB40E LFP) of 40Ah pouch type cell, which is energy cell. This cell is manufactured by the European Batteries. The performance parameter characteristics of cell is included in Table 8.

Nominal capacity (Ah)	40
Nominal Voltage (V)	3.2
Max. voltage (V)	3.65
Min. voltage (V)	2
Weight (kg)	.98
Nominal Energy (Wh)	128
Spec. Energy (Wh/kg)	130
Max. discharge current cont (A)	270
Peak Current discharge 10s (A)	180
Peak regen. Current 10s (A)	90
Peak spec. discharge power 10s (W/kg)	588
Peak discharge power 10s (W)	576

Table 8 - The performance parameter characteristics of cell.

Battery geometry, external and internal structures

The commercial lithium-particle batteries can be arranged by cell shape and part materials. The different types of batteries incorporate cylindrical, prismatic and pouch cells have key parts in a LIB, for example, cathode active material, the anode active material the current collector (aluminum and copper), the separator the electrolyte and the tab external packaging. Cylindrical cells have twisting wound structure and are simpler to fabricate with a decent mechanical stability. Be that as it may, they have generally a low packing energy density. Prismatic cells have jam roll or stacked layer structures with high packing energy density and are more costly to make. Pouch cells, which could be considered as thin prismatic cells within a flexible enclosure. They have stacked layer structure with higher energy density than the Cylindrical and Prismatic shaped cell, and give greater adaptability of the plan perspective and are moderately more affordable. Notwithstanding, they remain precisely powerless, and require a solid case for the module bundling, this load of three sorts of LIB incorporate a few single battery layer with a measurement of 100 microns. Each single battery layer contains various segments (cathode, anode, separator and electrolyte) and work as indicated by the alleged "extraction/inclusion" process.

Effect of temperature on the battery behaviors

A thermal management system for batteries is required on account of the best ideal temperatures of the batteries don't go along totally with the conceivable working temperatures of the vehicle. The best temperature range of surrounding temperature for Li ion batteries is arranged somewhere in the range of 25°C and 40°C [45], while the activity range of a vehicle is conceivable between - 30°C and 60°C relying upon the geographic areas and climatic zones.

Phenomena that happen when the temperature exceeds the prescribed limits are summed up in Table 9. Global trends of battery behaviors are identified with the chemistry, design and manufacturer of the battery package. Low temperature induces to the capacity drop and internal resistance raised due to the lower chemical activity. The increase in resistance will result in a higher heat generation. However, high temperature leads to an increase of the internal resistance, to self-discharge and in worst case to thermal runaway. These phenomena may decrease battery performance and lifetime.

Low temperature (<0°C)	<ul style="list-style-type: none"> - Capacity drop - Internal resistance increase
High temperature (>40°C)	<ul style="list-style-type: none"> - Internal resistance decrease - Accelerated aging phenomena - Higher self-discharge - Decomposition of electrolyte - Thermal runaway, safety considerations - Reduced life cycle

Table 9- The phenomena that happen when the temperature exceeds the prescribed limits.

Effect of cell design on the battery behaviors

Advanced research in the field of rechargeable energy storage (RESS) allowed to a wide use of large oversized, high-capacity Li-ion cells in PHEVs and EVs. This format has the feature in decreasing the number of cells in the module, expanding the capacity and diminishing the size and weight at the pack level. Increasing the current capacity during the charging/discharging process exposes an oversized battery to abuse and leads to erratic distributions of temperature, voltage, current density, and heat generation across the cell. Awful design and extreme operation conditions of large format cells may diminish battery performance and lifetime. Therefore, for the good cell design, it is necessary to avoid non-uniform distribution of the electrical and thermal parameters. The temperature differences within a cell and amongst the cells in battery pack should be smaller than 5°C [46]. Furthermore, the particle size and the electrode coating thickness have also a significant impact on battery behavior. Recently, Zhao et al [47] little coin cells give much preferable execution and energy density than large format cells, where uneven current density is observed, leading to lower utilization of the active material. In addition, the impact of the arrangements and the number of the current collecting tabs are investigated in the cases of wound design [48] and stacked layer design [49]. As a component From the number and location of the tabs, the electron paths become longer or shorter and thus cause the expand or diminish of the ohmic resistance responsible for the voltage loss. Interaction between the cooling systems and the design of the battery is expected to guarantee this consistency of temperature.

Battery Models

To create effective battery management system (BMS), designing the battery cell and dimensioning the cooling and heating systems, the improvement of an accurate model is essential. Three classifications of models are reported in the literature:

- The equivalent circuit model (ECM),
- The electrochemical models,
- The empirical model.

All these battery models are generally coupled with the thermal model. The ECM and the electrochemical models are the most generally utilized.

Electrical-thermal modeling

The coupling scheme between the electrical and thermal models with the model inputs and outputs are shown in Figure 18. The electrical parameters, such as the resistance and capacitance depend on the State of charge (SoC) and temperature. The resistance and the current are used to calculate the battery heat source. The calculating of the State of charge (SoC) depends on Coulomb counting method, where:

$$\text{SoC}(t) = \text{SoC}(t_0) + \frac{\int_{t_0}^{t_0+t} I_t d\tau}{Cn} \quad (1)$$

where

Cn the nominal capacity of the battery in (Ah).

I the current of charge or discharge in (A).

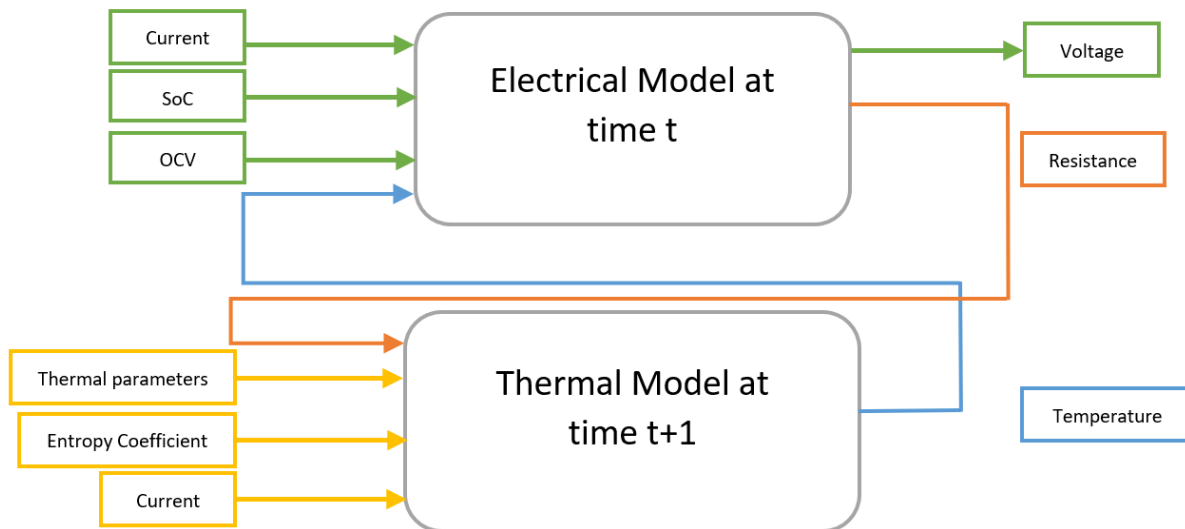


Figure 18- The coupling scheme between the electrical and thermal models.

Electrical Circuit Model (ECM)

Various ECM are developed and presented in the literature. The accuracy and precision of them relies upon the battery chemistry. Among the most applicable one, we can discover:

- Shepherd Model [50],
- Rint battery model [51]
- RC battery model [52],
- FreedomCar Battery model [53],
- Thévenin Battery model [53],
- Second order FreedomCar Battery Models [53].

The ECMs consists of electrical components such as capacitors, resistances (ohmic and polarization), and voltage sources (open circuit voltage). Figure 19 shows the voltage response of a lithium-ion cell after a pulse test, the voltage decreases in three parts:

- The first part corresponds to the ohmic loss without any time delay.
- The second part corresponds to the voltage loss caused by charge transfer runs after a time delay.
- The third part corresponds to the voltage loss by diffusion of lithium in the active material.

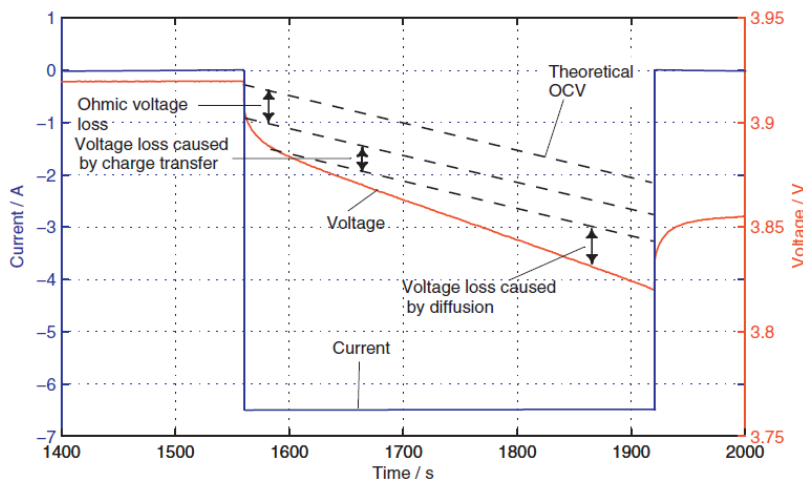


Figure 19- The voltage response of a lithium-ion cell after a pulse test.

These various phenomena are included in the ECM model. For example in Figure 20, the first order Thévenin battery model is shown, where:

- OCV illustrates the open circuit voltage of the battery
- R_o illustrates the ohmic resistance
- R_p illustrates the polarization resistance due to the charge transfer
- C_p illustrates the polarization capacitance in parallel with R_p
- VL illustrates the battery voltage

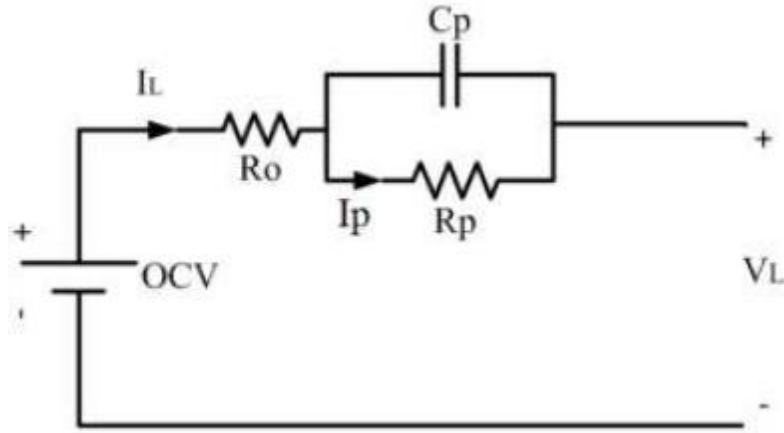


Figure 20- The first order Thévenin battery model.

The electrical parameters of these models can be separated by performing tests such as the HPPC (Hybrid pulse power characterization test) [54] in the time domain model or by using the electrochemical impedance spectroscopy (EIS) [55] in the frequency domain. These tests are combined with an assessment technique, such as generic algorithm (GA) optimization [56], nonlinear least squares curve fitting techniques [57] in order to remove the electrical parameters from the used model. These techniques can be utilized without the need to get to the innards of the battery cell. Afterwards, the battery model is created based on look-up tables with cell electrical parameters. As a function of the inputs (current, OCV (open circuit voltage)) as shown in Figure 21.

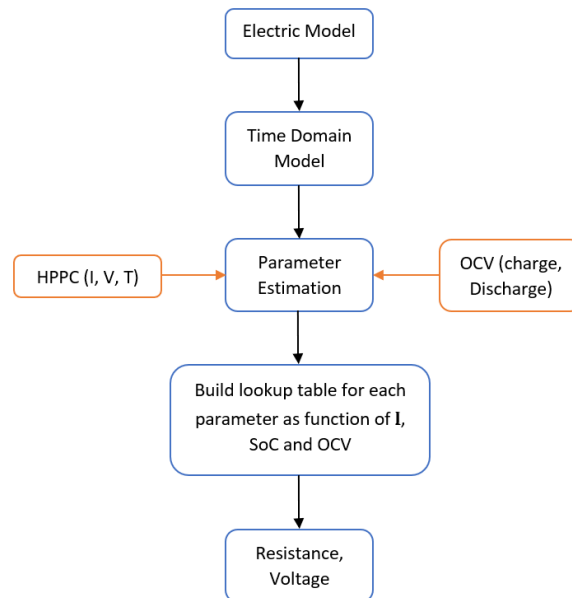


Figure 21- The Electric model process.

Thermal Model

The thermal model delivers the temperature distribution of the cell, which relies upon the electrical parameters and the operating conditions (current, cooling method and ambient temperature). The thermal model depends on the energy balance, taken in one, two or three-dimensional according to the geometric features of the battery. The heat source is derived from three main phenomena [43] :

- The reversible heat corresponding to the chemical reaction, showed by an entropy change.
- The irreversible heat including ohmic heat and polarization heat.
- The heat generated by side reactions, for example, corrosion reaction, overcharge, and chemical shorts.

The last point is for the most part disregarded. The irreversible heat is computed from the electrical parameters (internal and polarization resistances) including in the lookup table of the electrical model. While the reversible heat is computed from the entropy coefficient, based on the OCV change as a function of cell temperature [58].

To solve the electrical-thermal modeling, two types of techniques have been to considered in the literature: Analytical techniques give continuous solutions and can show explicitly how the parameters affect the solutions [59]. Several analytical techniques exist, such as Laplace transformation [60], separation of variables [61], Green's function [62], etc. Numerical techniques are performed dependent on complex models relying upon the design and the multidirectional heat transfer of the battery. They use many discretization techniques such as a finite differential method (FDM), finite volume method (FVM), the finite element method (FEM) and etc. To solve the energy balance equation, numerical methods are typically executed in commercial software packages such as ANSYS, etc. . . .

Many one-dimensional thermal equivalent circuit models (TECM) applied to cylindrical and prismatic cell have been developed in the literature [43], [63] ; they are more convenient for small cylindrical cells where the temperature gradient along the axial direction comparing to the radial direction is almost negligible. While the others multidimensional thermal models have been developed in the literature [63]. They are more appropriate for large cells where asymmetric temperature distribution arises from geometric effects and from the cooling method. One difficulty for developing precise battery thermal models is that the thermal parameters are difficult to obtain. Various techniques have been established, for example parameters assessment and measurement techniques.

In the estimation technique, two approaches have been utilized in the literature. The first one considered the active material as a continuous material with anisotropic properties that rely upon the layered directions. Typically the active material is assumed to comprise of several layers (anode, cathode, separator and current collectors). The thermal conductivity along and across the layers can be assessed as a function of the thicknesses (li) of the different layers and the thermal conductivity (ki) of the material comprising these layers as shown in Eq (2) and Eq (3). The density (ρ) and heat capacity (Cp) of the active material are determined similarly as a function of the density (ρi) and heat capacity ($Cp i$) of the material constituting these layers, as illustrated in Eq (4) and Eq (5).

$$\text{SoC}(t) = \text{SoC}(t_0) + \frac{\int_{t_0}^{t_0+t} I_t d\tau}{cn} \quad (1)$$

Thermal conductivity across the layers (kn):

$$K_n = \frac{\sum_i l_i}{\sum_i \frac{l_i}{k_i}} \quad (2)$$

Thermal conductivity along the layers (kt):

$$K_n = \frac{\sum_i l_i k_i}{\sum_i l_i} \quad (3)$$

Density (ρ) and thermal capacity (Cp) of the active material:

$$\rho = \frac{\sum_i l_i \rho_i}{\sum_i l_i} \quad (4)$$

$$Cp = \frac{\sum_i l_i Cp_i}{\sum_i l_i} \quad (5)$$

The material structure of the layers should be well known to obtain a good accuracy of this model. This is rarely the case in the competitive industry; the manufacturers do not want to uncover their secrets. The second estimation technique is depended on the solving of a first order thermal equivalent circuit model [64]. By applying a micro-pulse test, one can estimate the different thermal resistances. However, this method is achieved to estimate the thermal parameters in one direction and requires to insert a thermal sensor inside the battery in order to calculate the conductive resistance. The thermocouple embedded inside the battery can involve oxidation risks. The thermal parameter measurement can be defined by using accelerating rate calorimeter (ARC), differential scanning calorimeter (DSC), thermal impedance spectroscopy, hot disc method, flash method, etc. However, these devices are not cheap and available in laboratories specialized on material characterization.

Electrochemical-thermal modelling

The electrochemical or physics based model is a multidimensional model that includes the resolution of the physical and electrochemical variable at the different length scale (particle, electrode and cell levels) as shown in Figure 22. This model has been firstly developed by Doyle, Fuller and Newman [65] dependent on the porous electrode hypothesis.

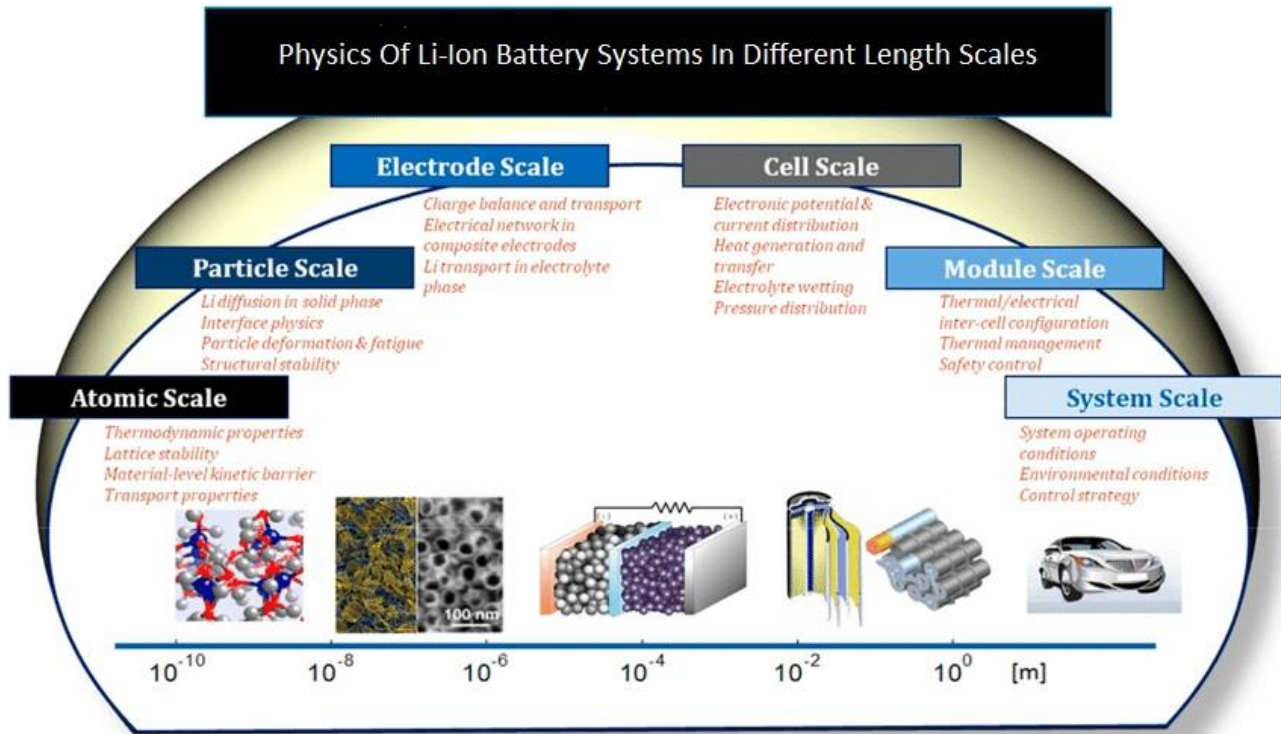


Figure 22- The physics of Li-ion battery systems in different length scales.

Electrochemical modeling methods are more suitable than the electrical modeling to investigate the battery designs, because they show a briefly relation between the electrochemical parameters and battery geometry and have a relatively high accuracy.

The main disadvantages of this model are the difficulty to obtain the required parameters, also long computational times because of the lot of effort of meshing. Most of the electrochemical parameters rely upon the temperature.

Many 1D electrochemical models are listed in the literature [66]. These are more appropriate for describing small-format batteries. They also provide average values for large-format batteries without taking into account the collector tabs. However, they are not sufficient to handle the issue of non-uniform thermal, electrical and electrochemical variable distributions observed in large-format cells. Recent advances in numerical simulation techniques applied to Li-ion batteries focus on the development of 2D axisymmetric and 3D electrochemical-thermal modeling [48], [67]. The multi-dimensional simulations are highly nonlinear and computationally demanding, and coupling electrochemical and thermal modeling represents an important step towards accurate simulation of the Li-ion battery. Most of the models in the literature use the electrochemical-thermal coupling model. As illustrated in Figure 23, the coupling

method 1 is performed by utilizing the volume-average temperature of the cell from the previous time step as inputs to update the electrochemical parameters and compute the heat source. This coupling method is less time and memory consuming. Little work centers around on the coupling method 2 [66]. This method shows results that are more precise with time consuming.

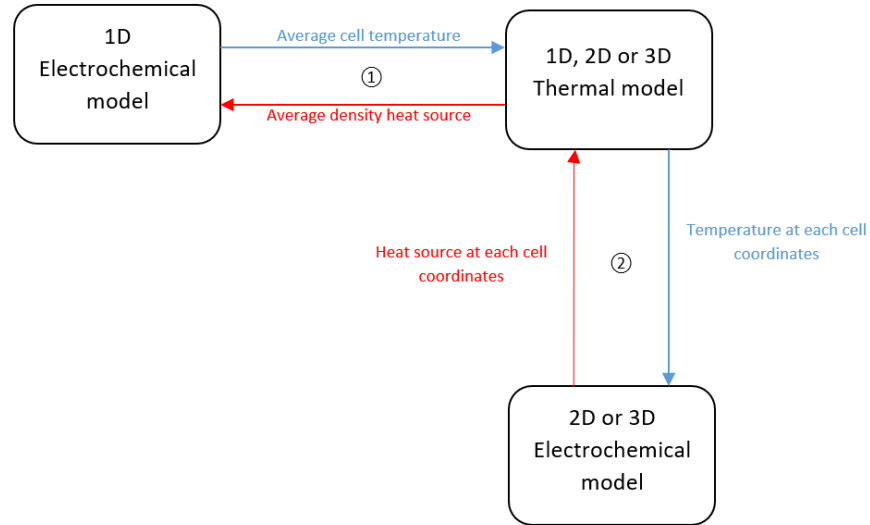


Figure 23- The types of coupling between electrochemical and thermal models.

In order to gain insight into large-scale battery behavior and to investigate the effect of the number of collecting tabs on the battery performance, the large portion of 2D and 3D electrochemical-thermal models are applied to the spirally wound design. However, little work is centered around stacked layered designs and the effect of the tab positioning on performance and variable distributions.

Chapter 4: Electrical –Thermal Model for Large Size Lithium-ion Cells

In this thesis we will develop two dimensional electrical-thermal in order to investigate and to analyze the temperature distribution over the battery surface. Then we will use the ANSYS FLUENT software to solve the model development. After that the model will validated by the experimental results. in addition, we will test the thermal behavior of the battery at different environmental conditions as well as during abuse conditions.

As mentioned previously, the temperature has a strong influence on the battery performance and safety. It is proposed also that the Electrical Circuit Model (ECM) is the most appropriate models that can be achieved in a BMS. Moreover, the electrical parameters greatly depend on the cell temperature, including in the ECM model. This input will obtain by using thermal models or by real time recording through a thermocouple. the knowing of the battery temperature distribution under all environmental conditions is important in order to keep the battery temperature on the safe range on one hand and on the other hand to increase its performance. The models for the Large and high capacity cells are not more suitable for the thermal parameter estimation of small capacity cells models. The Large and high capacity cells, as widely used in Battery Electric Vehicle (BEV) applications, are generally subject to heavy solicitation that can lead to non-uniform temperature distribution.

In [61], [63] we found in it that the large cells are more suitable in different 2D and 3D electrical-thermal models, they have been developed with known thermal parameters. So from this investigation, we found the possibility to avoid the insertion of thermal sensors inside the battery with developing a dedicated battery electro-thermal model that can be applied for any type of battery cell (scale and chemistry), with a new methodology to evaluate the battery thermal parameters in all directions. The main advantage of this model is the thermal parameters can be estimated by input and output signals (current voltage and cell surface temperature) without knowing the materials and layers composition, and then included these parameters in the CFD models.

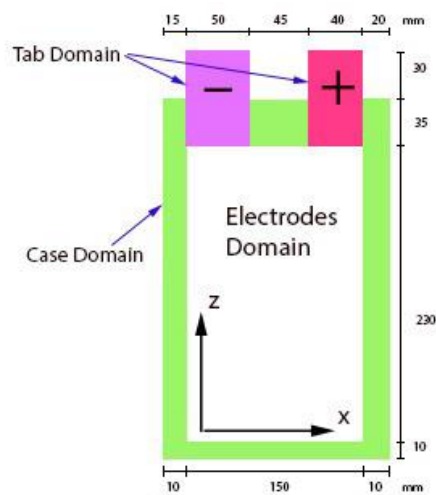


Figure 24- The pouch cell model with the size of the different domains.

the selected pouch cell is 40 Ah with chemistry LiFePO₄/graphite will develop to simulate the thermal behavior at different operating conditions. The heat generation and thermal properties are the input parameters. Furthermore, the thermal behavior of the proposed battery has been investigated at different environmental conditions as well as during the abuse conditions by using the ANSYS FLUENT software.

Thermal modelling

Model assumptions and geometry features

Generally, soft pouch cells for BEVs vary between 5 and 20 mm, depending on the battery cell capacity. The pouch cell model with the size of the different domains is shown in Figure 24. The material of domains is different. the thickness will be 12 mm; in the y-direction the heat development will be neglected. while the others two-dimensional(x,z) transient heat conduction equation enough to describe the thermal phenomena in the battery. Nevertheless, inside the battery the convective term will be neglected.

The thermal conductivities are anisotropic with a higher value along the x and z-directions, than the normal direction to the layers so the active material of the battery is supposed to consist of many single cell layers. Moreover, the thermal conductivity along x-direction is the same than the z-direction. Thus all various materials that the battery cell is consisting of, will set up as equivalent material to model.

Governing equations

Depend to the above presumption, the energy balance equation over a representative elementary volume (REV) in a battery, So the transient response of the temperature distribution for the 2D thermal modeling is possible to foresee formulated as:

- In the electrode and tabs domains:

$$k \left(\frac{\partial^2 T}{\partial x^2} + \frac{\partial^2 T}{\partial z^2} \right) + qg = \rho.Cp \frac{\partial T}{\partial t} \quad (6)$$

the heat generation for the electrodes domain, is given by:

$$qg = \frac{1}{V_{bat}} (R I^2 + (T \left[\frac{dE}{dT} \right]) I) \quad (7)$$

Where

qg is the volumetric heat generation in ($W.m^{-3}$),

R is the battery internal resistance in (Ω),

$\frac{dE}{dT}$ is the entropy coefficient in ($V.K^{-1}$),

I is the applied current (negative in discharge and positive in charge) in (A).

For the Tab domain, the heat generation is given by:

$$q_g = \frac{R^* I^2}{V_{bat}} \quad (8)$$

$$R^* = \rho^* \frac{l}{S} \quad (9)$$

- In case domains

$$\lambda \left(\frac{\partial^2 T}{\partial x^2} + \frac{\partial^2 T}{\partial z^2} \right) = \rho \cdot C_p \frac{\partial T}{\partial t} \quad (10)$$

Where

R^* is the electrical resistance in (Ω),

ρ^* is the electrical resistivity in (Ωm),

l is the length in (m),

S is the cross section in (m^2),

V_{tab} is the volume of the corresponding tab in (m^3)

Also,

ρ is the average density in ($kg \cdot m^{-3}$) which is equal to 2224 ($kg \cdot m^{-3}$),

C_p is the average specific heat in ($J \cdot kg^{-1} \cdot K^{-1}$),

λ is the average thermal conductivity along the x-direction and z-direction in ($W \cdot m^{-1} \cdot K^{-1}$).

Boundary conditions

The boundary conditions taken from the both convection heat and contributions of radiation and the conductivity heat flux from the battery surface to the surrounding:

$$q_s = -\lambda \left(\frac{\partial T}{\partial x} + \frac{\partial T}{\partial y} \right) |_{boundaries} = (h_{rad} + h_{conv})(T - T_a) \quad (11)$$

With

$$h_{rad} = \epsilon \sigma (T^2 - T_a^2) (T - T_a) \quad (12)$$

- but at this type of boundary, we have two domains of cell made of different material and the continuity is applied as follows:

$$\lambda \left(\frac{\partial T}{\partial x} + \frac{\partial T}{\partial y} \right) |_{domain 1} = \lambda \left(\frac{\partial T}{\partial x} + \frac{\partial T}{\partial y} \right) |_{domain 2} \quad (13)$$

Where

h_{rad} is the radiative heat transfer in ($W \cdot m^{-2} \cdot K^{-1}$),

h_{conv} is the convective heat transfer in ($W \cdot m^{-2} \cdot K^{-1}$),

ϵ is the emissivity of the cell surface which is equal to 1 because the battery has been painted black (-),

σ is the Stefan–Boltzmann constant which is ($5.669 \cdot 10^{-8} W \cdot m^{-2} \cdot K^{-4}$),

T is the battery surface temperature in (K°),

T_a is the ambient temperature in (K°).

The case domains are made by aluminum; all related thermal parameters of this domain are taken from [68]. The thermal parameters used in the tab domains are summarized in Table 10.

Properties	Positive tab (aluminum) and case domain	Negative tab (copper)
ρ ($kg.m^{-3}$)	2692	8887
λ ($W.m^{-1}.K^{-1}$)	179.9	344.5
C_p ($J.kg^{-1}.K^{-1}$)	880	385

Table 10- The thermal parameters used in the tab domains.

The electrical resistance of the aluminum positive tab is 4.26 m Ω and the electrical resistance of the copper negative tab is 1.08 m Ω . These resistances are computed from the Eq (9) with taken the tab dimensions and the resistivity value. Therefore, the heat generated at the positive tab is higher than at the negative tab. Knowing the heat generation variation and thermal parameters, we will use the finite volume numerical to solve the energy balances by ANSYS Fluent software.

Heat generation measurement

The expression of heat source is gotten from E. Pawlikowski. [69] by applying the first law of thermodynamic energy balance on a cell control volume. Two fundamental of heat source are considered: the first represents the entropic heat from the reaction, and the second is the over potential heat due to ohmic losses in the cell, the charge-transfer over potentials at the interface and the mass transfer limitations. The heat source from mixing effects and phase change are neglected in this expression. The parameters which allow us to determine the heat source are the internal resistance and the entropy coefficient which have been extracted experimentally.

Internal resistance measurement

The measurement method of the internal resistance is described in [70], [71]. Firstly, to ensure constant battery temperature the battery is first placed in a climatic chamber to ensure constant battery temperature. Then, we will apply the extended hybrid pulse power characterization (HPPC) test, whereby at a specific SoC, different charge and discharge current pulse rates of 10 seconds, with a rest of 300 seconds in between is applied. The test procedure is repeated at different environment temperatures. In this work, the Internal resistance measured experimentally. Based on the Levenberg-Marquardt minimization algorithm applied to the first order Thévenin model, the internal resistance is estimated based on the methodology described in Figure 25 .

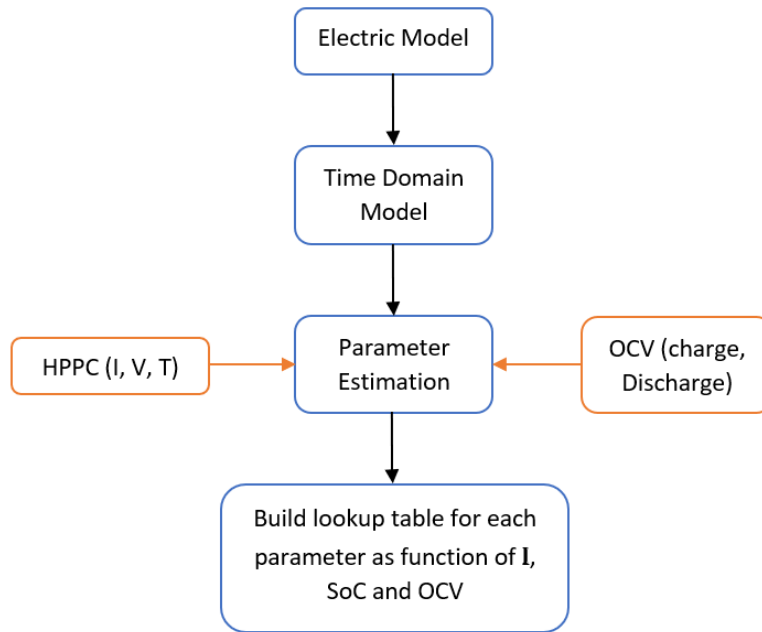


Figure 25- The pouch cell model with the size of the different domains.

the HPPC is performed at different temperatures (0°C, 10°C and 30°C), current rates (0.5It, 1It and 2It) and SoC (100% to 0% by step of 5%). Where the It represents the current value corresponding to the battery capacity in Ah and in our case 1It corresponds to 40 A. The variation of internal resistance as a function of SoC and temperature at 0.5It, 1It and 2It charge and discharge current rates are plotted in Figure 26, Figure 27, Figure 28, Figure 29, Figure 30 and Figure 31. Between 100% and 90% SoC, the internal resistance decreases directly with the decrease of SoC. From 90% and downwards the internal resistance maintain more less stable. Below 20%, the resistance increases but at low temperatures, due to the increase of the electrolyte's viscosity the internal resistance increases, which is limiting the ionic transport reaction speed. Also, as shown that the increasing of the current rate leads to decrease the internal resistance in figures.

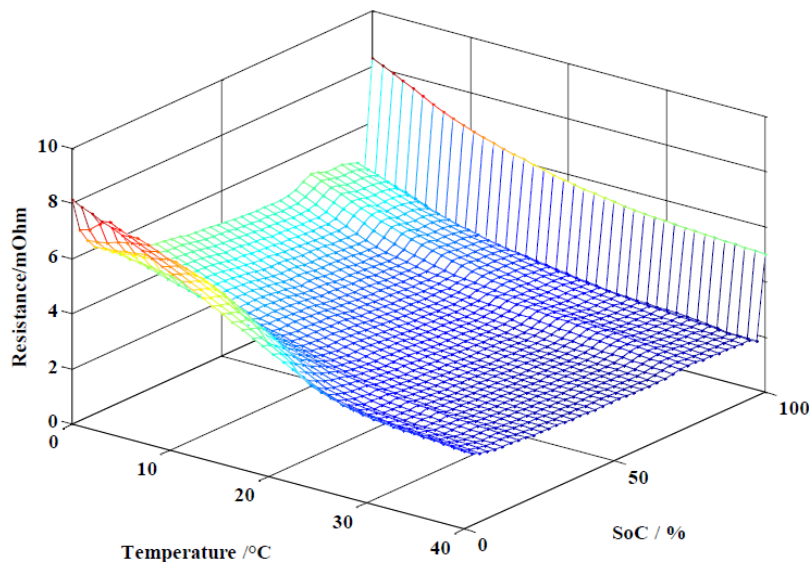


Figure 26- Internal resistance of charge as a function of SoC and Temperature at 0.5 It current rate.

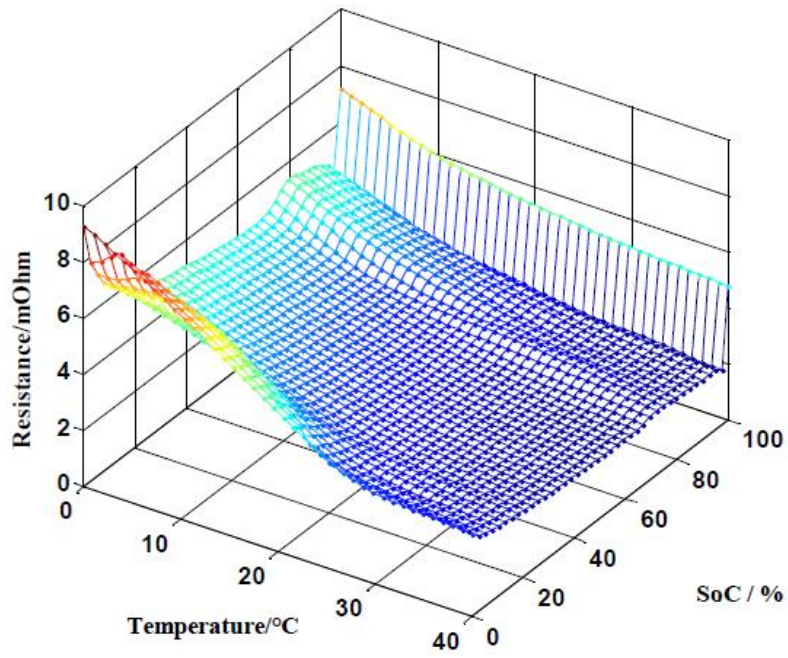


Figure 27- Internal resistance of discharge as a function of SoC and Temperature at 0.5 It current rate.

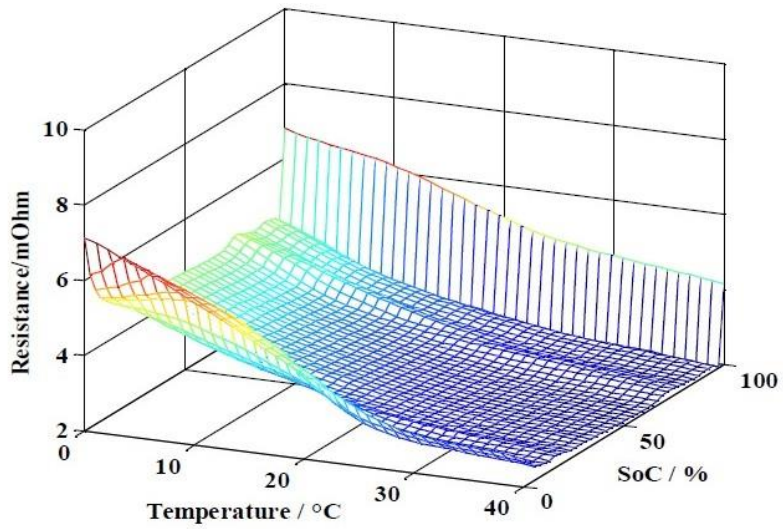


Figure 28- Internal resistance of charge as a function of SoC and Temperature at 1 It current rate.

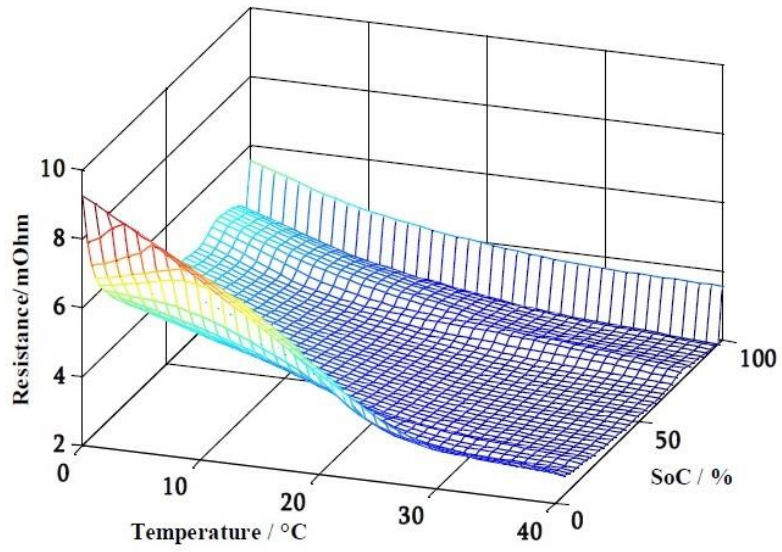


Figure 29- Internal resistance of discharge as a function of SoC and Temperature at 1 It current rate.

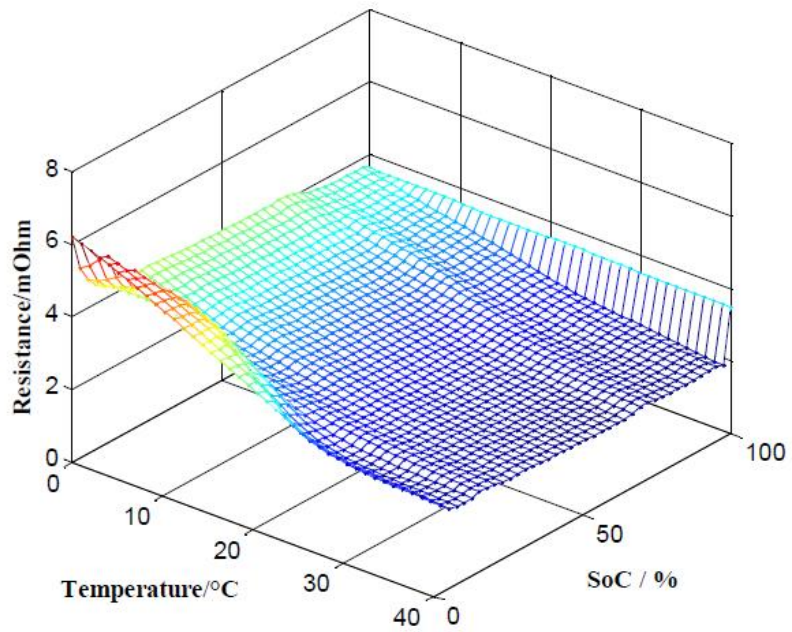


Figure 30- Internal resistance of charge as a function of SoC and Temperature at 2 It current rate.

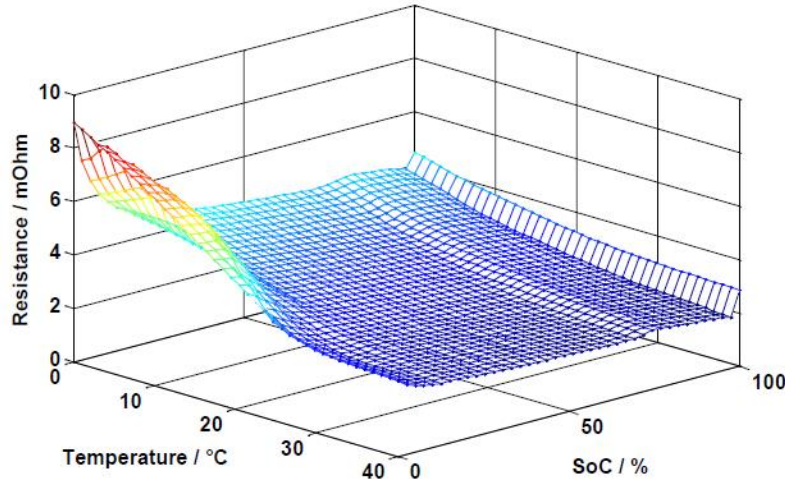


Figure 31- Internal resistance of discharge as a function of SoC and Temperature at 2 It current rate.

Entropy coefficient measurement

The entropy coefficient is based on the open circuit voltage (OCV) measurement as a function of battery temperature at different SoC levels. In this thesis methods, the voltage relaxation method [72] is used to measure the OCV. The OCV measurement was applied during the charge, discharge process as follows:

- Firstly, the battery charged at 0.5 It up to 3.65V, followed by a constant voltage charge of 3.65V up to 1A, corresponding to a SoC of 100%.
- With a programmable climatic chamber, the OCV in discharge measured at different temperatures (10°C, 2°C, 15°C, and 30°C). For each temperature level, 3h was needed to ensure constant battery temperature.
- The battery discharged at 0.5 It by a step of 10% of SOC.
- The battery left in open circuit for about 3h relaxation at each SoC in order to reach a relatively stable state. Then, the OCV measurement as a function of temperature was repeated.

The OCV measurement repeated in charge process by discharging completely the battery at 1/2 It up to the cutoff voltage 2V, corresponding to a SoC of 100%. After relaxation time of 3h the OCV measured at different temperatures. The OCV in charge is as a function of temperature at 0% of SoC, where at the end of each temperature variation the steady state was reached. therefore, the battery charged at 0.5 It by a step of 10% of SOC and the OCV in charge was measured at different temperatures at each SoC. Experimentally The entropy coefficient for a given SoC obtained from the slope of the open circuit voltage (OCV) curve as a function of temperature. At each SoC (90% to 0% by step of 10%), This calculation procedure is repeated during both charging and discharging. The entropy coefficient as a function of SoC during charge and discharge process have differences between both because of the hysteresis of the open circuit voltage (OCV). The result observed for various lithium-ion batteries [70], and is more cleared at low SoC [72]. The reversible heat is dominant respect to the irreversible heat for low charge or discharge current rates. Relating to the reversible heat formula ($T \left[\frac{dE}{dT} \right] I$), the sign of the current (positive in charge and negative in discharge) and the sign of the entropy coefficient will define if this term will be positive or negative. If the reversible heat is positive, therefore the chemical reactions are exothermic otherwise, they are endothermic. Physically, when the chemical bonds of the reactants are higher than those of the product the endothermic reaction is existed, then extra energy should be absorbed from the external environment to create new bonds. While the opposite situation occurs during exothermic reaction. Generally, the entropy measures the degree of disorder in a system at the

microscopic level. So the higher entropy, the less its elements are ordered and the higher the system energy. But in this work we got the Entropy coefficient theoretically as a function of SoC by applying this formula :

$$\frac{dU_p}{dT} = -0.35376\theta_p^8 + 1.3902\theta_p^7 - 2.2585\theta_p^6 + 1.9635\theta_p^5 - 0.98716\theta_p^4 + 0.28857\theta_p^3 - 0.046272\theta_p^2 + 0.0032158\theta_p - 1.9186 \quad (14)$$

$$\frac{dU_n}{dT} = -344.1347148 \times \frac{e^{(-32.9633287\theta_n + 8.316711484)}}{1 + 749.0756003e^{(-32.9633287\theta_n + 8.316711484)}} - 0.8520278805\theta_n + 0.362299229\theta_n^2 + 0.2698001697 \quad (15)$$

Where

$\frac{dU_j}{dT}$ is the Entropy coefficient in (-)
 θ_j is the state of charge (SoC) in (-) and ($j = p, n$)

Battery thermal model parameters

As the dynamic performances of cells during operation are related to their temperature, an accurate thermal model is necessary to explore the battery behavior during operation and in advance. As the battery cell consists of a combination of materials and layers not accurately mentioned and it is considered as a “black-box”, thermal parameters have to be estimated from the input and output signals. Practically, the current, voltage and surface temperature of the battery cell only can be measured. Electrical parameters are evaluated related to the first order Cauer network, where the energy balance is represented by an equivalent circuit in each direction of the cell, as shown in Figure 32, where P_g is the total heat generation, R_{th} is the conductive thermal resistance and R_{con} represents the convection and radiation thermal resistance and C_p is the thermal capacitance. This model has less presumption comparing to certain models utilized in the literature [64] where the thermal sensor inserted inside the battery in order to calculate the thermal resistance R_{th} and also these models assumed an ideal condition that the all power generated by the battery goes through the normal direction. Moreover, because of the shape of prismatic or pouch cell the dissipated power is not just released through the normal front and back directions to the ambient ($T_{s,front}$ and $T_{s,Back}$ as shown in Figure 32) but also along the surface directions to the ambient (T_{s1} , T_{s2} , T_{s3} and T_{s4} as shown in Figure 32) so the previous presumptions are only valid for cylindrical battery shape. So the best way is to insert the thermocouple inside the battery.

So Firstly to estimate the thermal battery model parameters, a micro-pulse test is used current rate at 3 It until the battery surface temperature reached the steady state and it found the differences between the temperature at each surface did not exceed 1 °C. According to these results, the emitted power generation percentage along each direction is determined. It defined as the part of heat generated through the front direction (P1), the right direction(P2) and the down direction(P3). The heat accumulation is equal to zero at steady state, and from Figure 32, the energy balance can be :

$$P_g = 2. P1 + 2. P2 + 2. P3 \quad (16)$$

Where

P_g is the generated heat in [W].

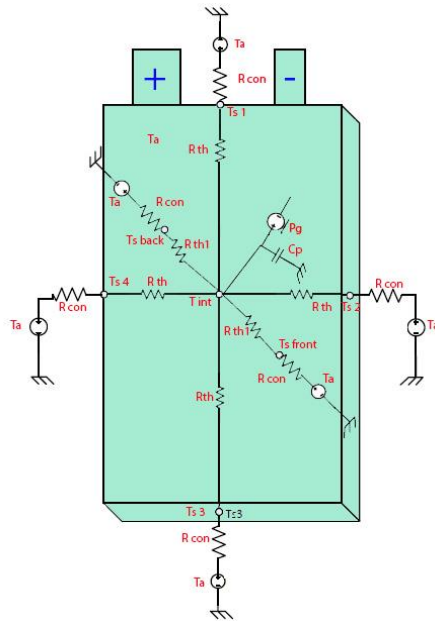


Figure 32- The Cauer network.

Relating to the Newton's law of cooling, the rate of heat loss of a body is directly proportional to the difference in the temperatures ΔT between the surface and its surroundings, the total heat transfer coefficient h ($W/m^2 K$) and surface. ΔT_1 , ΔT_2 and ΔT_3 are the temperature differences linked to the direction of P_1 , P_2 and P_3 , and A_1 , A_2 and A_3 are the related areas. Then at the steady state, due to the differences between the temperature at each surface did not exceed $1^\circ C$ and the Figure 32. the following equations:

$$P_1 = hA_1\Delta T_1; P_2 = hA_2\Delta T_2; P_3 = hA_3\Delta T_3 \quad (17)$$

$$\Delta T_1 = \Delta T_2 = \Delta T_3 \quad (18)$$

These equations also can be expressed as:

$$\frac{P_2}{P_1} = \frac{A_2}{A_1}$$

$$\frac{P_3}{P_1} = \frac{A_3}{A_1}$$

(19)

Substitution of (19) in (17):

$$P_g = 2 \cdot P_1 + 2 \frac{A_2}{A_1} P_1 + 2 \frac{A_3}{A_1} P_1 \quad (20)$$

relating to the cell dimensions:

$$P_1 = 0.45 P_g; P_2 = 0.03 P_g; P_3 = 0.02 P_g \quad (21)$$

In each direction the calculated percentage of heat generated is used to estimate the associated thermal parameters with the least-square curve fitting method.

Chapter 5: Simulation and Results

All equations are simultaneously solved numerically in ANSYS FLUENT. for the governing equations which are nonlinear, the precision of the calculation relies on the solver and mesh so the entire computational domain is used 25,000 structured elements. The simulation occurred at different operating conditions and current rates. The modeling of thermal distributions at different time steps of 0.5 It, 1 It (charge and discharge) and at 4 It for discharge for the period 15,30 and 45 minutes.

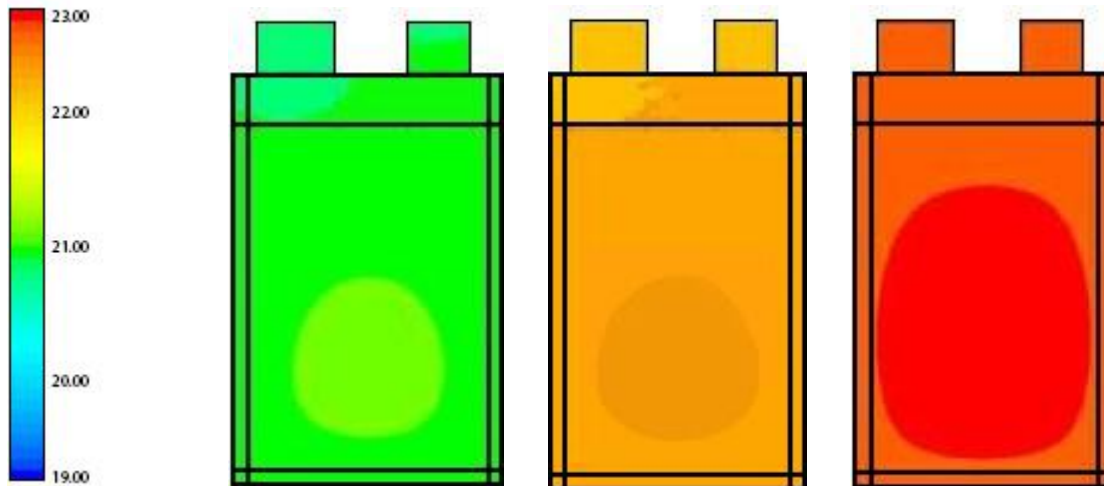


Figure 33- Thermal distributions based on experimental thermal imager and modeling at 0.5 It charge current rate at 20°C of environment temperature.

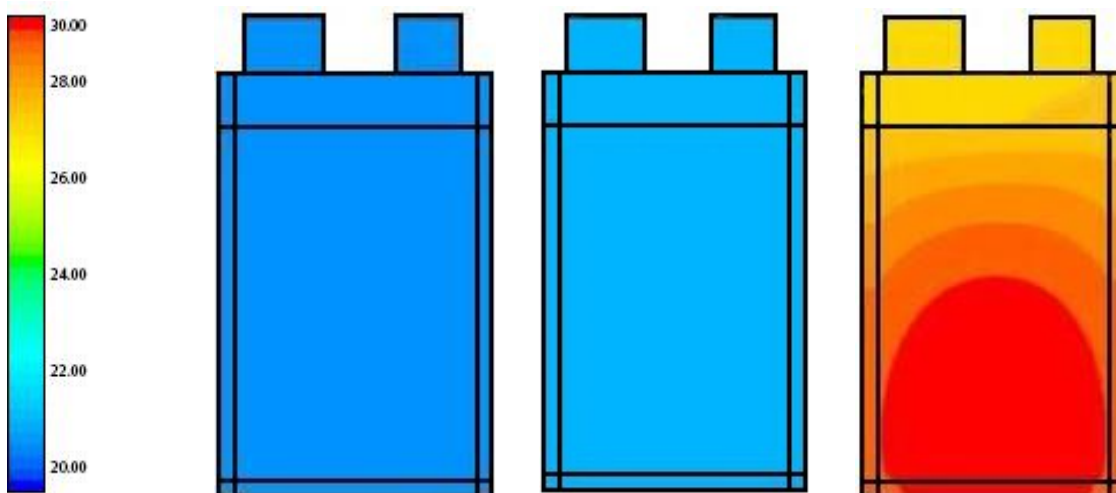


Figure 34- Thermal distributions based on experimental thermal imager and modeling at 0.5 It discharge current rate at 20°C of environment temperature.

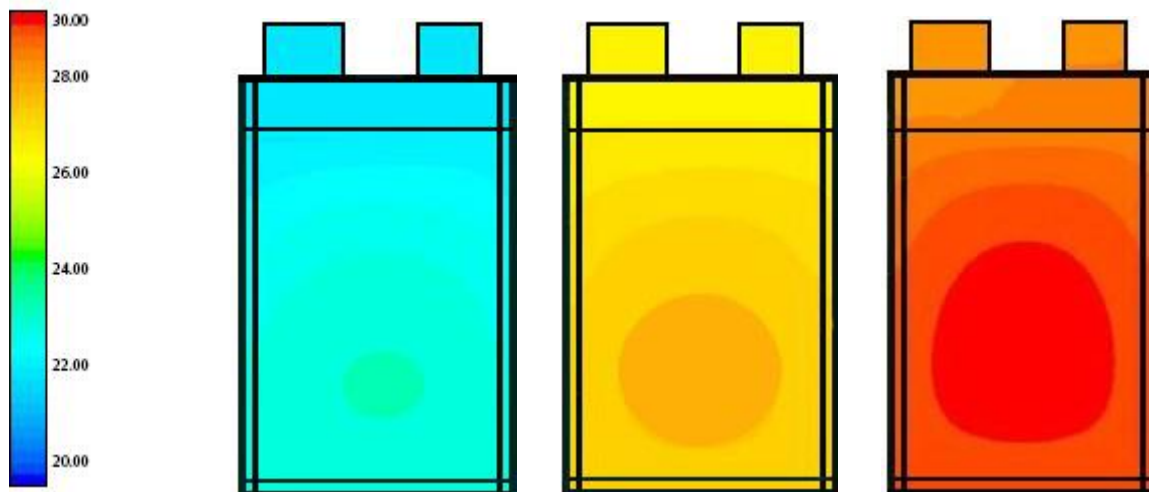


Figure 35- Thermal distributions based on experimental thermal imager and modeling at 1 It charge current rate at 20°C of environment temperature.

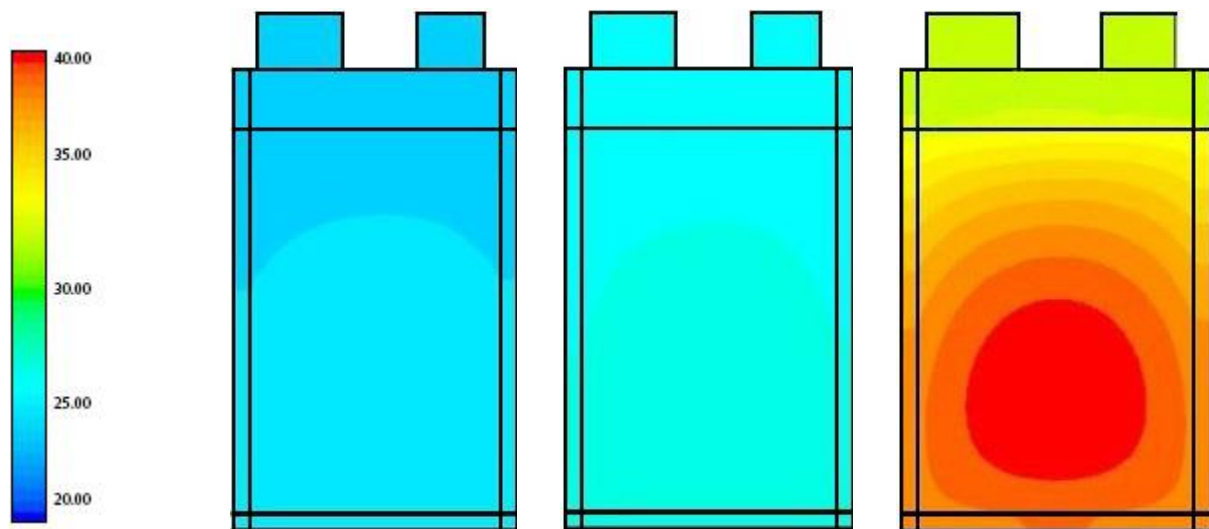


Figure 36- Thermal distributions based on experimental thermal imager and modeling at 1 It discharge current rate at 20°C of environment temperature.

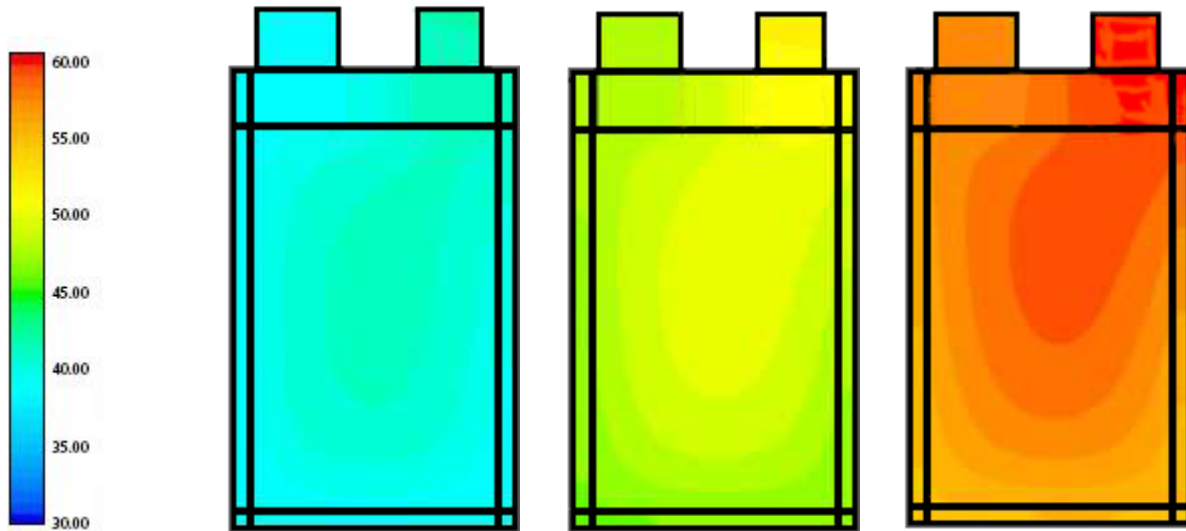


Figure 37- Thermal distributions based on experimental thermal imager and modeling at 4 It discharge current rate at 20°C of environment temperature.

Chapter 6: Conclusions

In this thesis, the large size of Li-ion pouch battery is developed in 2D-thermal model which is capable to foresee the surface temperature distribution of the battery at different operating conditions. The battery thermal parameter estimation is developed to evaluate the thermal parameters by using the first order Cauer model. It has been noticed that the battery temperature rises by increasing the current rate because the heat generation in the tab domains and electrodes are increased. Moreover, as shown in the temperature distribution at high discharge rate ($4 I_t$), the maximum temperature is located near the positive tab due to the high amount of heat generated at the positive tab, because of the resistivity of aluminum is higher than to the copper (at the negative tab). Moreover, at high current rate more than $1 I_t$ the generated heat is higher than the dissipated heat and the highest temperature is located near the positive tab. However, at low current rate, the highest temperature is located at the middle of the cell.

Publication bibliography

- [1] "IEEE Medal for Environmental and Safety Technologies Recipients". IEEE Medal for Environmental and Safety Technologies. Institute of Electrical and Electronics Engineers. Retrieved 29 July 2019.
- [2] National Institute for Materials Science (14-Apr-21): NIMS Award Goes to Koichi Mizushima and Akira Yoshino | NIMS. Available online at <https://www.nims.go.jp/eng/news/press/2016/10/201610120.html>, updated on 14-Apr-21, checked on 11-May-21.
- [3] Yoshio Nishi (11-May-21): National Academy of Engineering. Available online at <https://www.nae.edu/105800/Yoshio-Nishi>, updated on 11-May-21, checked on 11-May-21.
- [4] Heller, Adam (25 November 1975). "Electrochemical Cell". United States Patent. Retrieved 18 November 2013.
- [5] Zanini, M.; Basu, S.; Fischer, J. E. (1978). "Alternate synthesis and reflectivity spectrum of stage 1 lithium—graphite intercalation compound". *Carbon*. **16** (3): 211–212. doi:[10.1016/0008-6223\(78\)90026-X](https://doi.org/10.1016/0008-6223(78)90026-X).
- [6] [US 4304825](#), Basu; Samar, "Rechargeable battery", issued 8 December 1981, assigned to Bell Telephone Laboratories
- [7] Godshall, N.A.; Raistrick, I.D.; Huggins, R.A. (1980). "Thermodynamic investigations of ternary lithium-transition metal-oxygen cathode materials". *Materials Research Bulletin*. **15** (5): 561. doi:[10.1016/0025-5408\(80\)90135-X](https://doi.org/10.1016/0025-5408(80)90135-X).
- [8] International Meeting on Lithium Batteries, Rome, 27–29 April 1982, C.L.U.P. Ed. Milan, Abstract #23
- [9] "[Rachid Yazami](#)". [National Academy of Engineering](#). Retrieved 12 October 2019.
- [10] Novák, P.; Muller, K.; Santhanam, K. S. V.; Haas, O. (1997). "Electrochemically Active Polymers for Rechargeable Batteries". *Chem. Rev.* **97** (1): 271–272. doi:[10.1021/cr941181o](https://doi.org/10.1021/cr941181o). PMID [11848869](https://pubmed.ncbi.nlm.nih.gov/11848869/).
- [11] Nigrey, Paul J (1981). "Lightweight Rechargeable Storage Batteries Using Polyacetylene (CH)_x as the Cathode-Active Material". *Journal of the Electrochemical Society*. **128** (8): 1651. doi:[10.1149/1.2127704](https://doi.org/10.1149/1.2127704).
- [12] Godshall, N. A.; Raistrick, I. D. and Huggins, R. A. [U.S. Patent 4,340,652](#) "Ternary Compound Electrode for Lithium Cells"; issued 20 July 1982, filed by Stanford University on 30 July 1980.
- [13] Thackeray, M. M.; [David, W. I. F.](#); Bruce, P. G.; Goodenough, J. B. (1983). "Lithium insertion into manganese spinels". *Materials Research Bulletin*. **18** (4): 461–472. doi:[10.1016/0025-5408\(83\)90138-1](https://doi.org/10.1016/0025-5408(83)90138-1).
- [14] [US 4668595](#), Yoshino; Akira, "Secondary Battery", issued 10 May 1985, assigned to Asahi Kasei
- [15] Manthiram, A.; Goodenough, J. B. (1989). "Lithium insertion into Fe₂(SO₄)₃ frameworks". *Journal of Power Sources*. **26** (3–4): 403–408. Bibcode:[1989JPS...26..403M](#). doi:[10.1016/0378-7753\(89\)80153-3](https://doi.org/10.1016/0378-7753(89)80153-3).
- [16] Masquelier, Christian; Croguennec, Laurence (2013). "Polyanionic (Phosphates, Silicates, Sulfates) Frameworks as Electrode Materials for Rechargeable Li (or Na) Batteries". *Chemical Reviews*. **113** (8): 6552–6591. doi:[10.1021/cr3001862](https://doi.org/10.1021/cr3001862). PMID [23742145](https://pubmed.ncbi.nlm.nih.gov/23742145/).
- [17] "[Yoshio Nishi](#)". [National Academy of Engineering](#). Retrieved 12 October 2019.

- [18] Padhi, A.K., Naujundaswamy, K.S., Goodenough, J. B. (1996) "LiFePO₄": a novel cathode material for rechargeable batteries". *Electrochemical Society Meeting Abstracts*, 96-1, p. 73
- [19] C. S. Johnson, J. T. Vaughey, M. M. Thackeray, T. E. Bofinger, and S. A. Hackney "Layered Lithium-Manganese Oxide Electrodes Derived from Rock-Salt Li_xMnyO_z (x+y=z) Precursors" 194th Meeting of the Electrochemical Society, Boston, MA, Nov.1-6, (1998)
- [20] Chebiam, R. V.; Kannan, A. M.; Prado, F.; Manthiram, A. (2001). "Comparison of the chemical stability of the high energy density cathodes of lithium-ion batteries". *Electrochemistry Communications*. **3** (11): 624–627. doi:10.1016/S1388-2481(01)00232-6.
- [21] [US US6677082](#), Thackeray, M; Amine, K. & Kim, J. S., "Lithium metal oxide electrodes for lithium cells and batteries".
- [22] [US US6964828 B2](#), Lu, Zhonghua, "Cathode compositions for lithium-ion batteries".
- [23] *"In search of the perfect battery"* (PDF). *The Economist*. 6 March 2008. Archived from [the original](#) (PDF) on 27 July 2011. Retrieved 11 May 2010.
- [24] Chung, S. Y.; Bloking, J. T.; Chiang, Y. M. (2002). "Electronically conductive phospho-olivines as lithium storage electrodes". *Nature Materials*. **1** (2): 123–128. Bibcode:2002NatMa...1..123C. doi:10.1038/nmat732. PMID 12618828. S2CID 2741069.
- [25] Song, Y; Zavalij, PY; Whittingham, MS (2005). "ε-VOPO₄: electrochemical synthesis and enhanced cathode behavior". *Journal of the Electrochemical Society*. **152** (4): A721 A728. Bibcode:2005JEIS..152A.721S. doi:10.1149/1.1862265.
- [26] BASF breaks ground for lithium-ion battery materials plant in Ohio, October 2009.
- [27] [Monthly battery sales statistics](#). Machinery statistics released by the Ministry of Economy, Trade and Industry, March 2011.
- [28] ["IEEE Medal for Environmental and Safety Technologies Recipients"](#). *IEEE Medal for Environmental and Safety Technologies*. Institute of Electrical and Electronics Engineers. Retrieved 29 July 2019.
- [29] ["Lithium Ion Battery Pioneers Receive Draper Prize, Engineering's Top Honor"](#) Archived 3 April 2015 at the [Wayback Machine](#), University of Texas, 6 January 2014.
- [30] ["At long last, new lithium battery tech actually arrives on the market \(and might already be in your smartphone\)"](#). ExtremeTech. Retrieved 16 February 2014.
- [31] ["NIMS Award Goes to Koichi Mizushima and Akira Yoshino"](#). *National Institute for Materials Science*. 14 September 2016. Retrieved 9 April 2020.
- [32] Qi, Zhaoxiang; Koenig, Gary M. (16 August 2016). "High-Performance LiCoO₂Sub-Micrometer Materials from Scalable Microparticle Template Processing". *ChemistrySelect*. **1** (13): 3992–3999. doi:10.1002/slct.201600872.
- [33] ["The Nobel Prize in Chemistry 2019"](#). *Nobel Prize*. Nobel Foundation. 2019. Retrieved 1 January 2020.
- [34] "The Four Components of a Li-ion Battery".samsungsdi.
- [35] Zhang, J.; Zhang, X.; Hou, Z.; Zhang, L.; Li, C. Uniform SiO_x/graphene composite materials for lithium ion battery anodes. *J. Alloys Compd.* **2019**, 809, 151798, DOI: 10.1016/j.jallcom.2019.151798 .

- [36] "How does a lithium-Ion battery work? ".letstalkscience.ca/educational-resources.
- [37] "Types of Lithium-ion" batteryuniversity.com/article/bu-205-types-of-lithium-ion.
- [38] Di A.K. Maini, Nakul Maini "All in One Electronics Simplified", ISBN13:9789386173393.
- [39] "overview-about-prismatic-cell", labkarts.com/overview-about-prismatic-cell/
- [40] "summary table of lithium based batteries" himaxelectronics.com/summary-table-of-lithium-based-batteries-2/
- [41] P. Van den Bossche, F. Vergels, J. Van Mierlo, J. Matheys, and W. Van Autenboer, "SUBAT: An assessment of sustainable battery technology," J. Power Sources, vol. 162, no. 2, pp. 913–919, Nov. 2006.
- [42] J. Axsen, K. S. Kurani, and A. Burke, "Are batteries ready for plug-in hybrid buyers?," Transp. Policy, vol. 17, no. 3, pp. 173–182, May 2010.
- [43] S. Al Hallaj, H. Maleki, J. S. Hong, and J. R. Selman, "Thermal modeling and design considerations of lithium-ion batteries," J. Power Sources, vol. 83, no. 1–2, pp. 1–8, Oct. 1999.
- [44] L. Lu, X. Han, J. Li, J. Hua, and M. Ouyang, "A review on the key issues for lithium-ion battery management in electric vehicles," J. Power Sources, vol. 226, pp. 272–288, Mar. 2013.
- [45] D. Linden and T. B. Reddy, HANDBOOK OF BATTERIES.
- [46] A. A. Pesaran, "Battery thermal models for hybrid vehicle simulations," J. Power Sources, vol. 110, pp. 377–382, 2002.
- [47] W. Zhao, G. Luo, and C.-Y. Wang, "Effect of tab design on large-format Li-ion cell performance," J. Power Sources, vol. 257, pp. 70–79, Jul. 2014.
- [48] K.-J. Lee, K. Smith, A. Pesaran, and G.-H. Kim, "Three dimensional thermal, electrical, and electrochemical-coupled model for cylindrical wound large format lithium-ion batteries," J. Power Sources, vol. 241, pp. 20–32, Nov. 2013.
- [49] U. S. Kim, C. B. Shin, and C.-S. Kim, "Effect of electrode configuration on the thermal behavior of a lithium-polymer battery," J. Power Sources, vol. 180, no. 2, pp. 909–916, Jun. 2008.
- [50] O. Tremblay, L. A. Dessaint, and A. Dekkiche, "A generic battery model for the dynamic simulation of hybrid electric vehicles." Proceedings VPPC 2007, Texas, USA, 2007.
- [51] Y. Tang, "On the feasibility of hybrid battery/ultracapacitor energy storage systems for next generation shipboard power systems," Proc. VPPC 2010, 2010.
- [52] V. H. Johnson, A. A. Pesaran, and B. Court, "Temperature-Dependent Battery Models for High-Power Lithium-Ion Batteries," in EVS 17, 2000, pp. 1–15.
- [53] U. S. D. S. of Energy, "FreedomCAR Battery Test Manual For IDAHO." U.S. Department Secretary of Energy, 2003.
- [54] P. Van den Bossche, N. Omar, A. Samba, M. Al Sakka, H. Gualous, and J. Van Mierlo, "The Challenge of PHEV Battery Design and the Opportunities of Electrothermal Modeling," in Lithium-Ion Batteries: Advances and Applications, Elsevier 2., G. PISTOA, Ed. Amsterdam: Elsevier B.V, 2014, pp. 249–268.
- [55] M. Dubarry and B. Y. Liaw, "Development of a universal modeling tool for rechargeable lithium batteries," J. Power Sources, vol. 174, no. 2, pp. 856–860, Dec. 2007.

- [56] Y. Hu, S. Yurkovich, Y. Guezennec, and B. J. Yurkovich, "Electro-thermal battery model identification for automotive applications," *J. Power Sources*, vol. 196, no. 1, pp. 449–457, Jan. 2011.
- [57] E. K. L. Long, P. Bauer, "A practical circuit-based model for Li-ion battery cells in electric vehicle applications," in *Telecommunications Energy Conference (INTELEC)*, 2011, pp. 1–9.
- [58] S. Al-hallaj and J. R. Selman, "Thermal modeling of secondary lithium batteries for electric vehicle / hybrid electric vehicle applications," *J. Power Sources*, vol. 110, pp. 341–348, 2002.
- [59] G. G. Botte, V. R. Subramanian, and R. E. White, "Mathematical modeling of secondary lithium batteries," *Electrochim. Acta*, vol. 45, no. 15–16, pp. 2595–2609, May 2000.
- [60] D. B. P. Huynh, D. J. Knezevic, and A. T. Patera, "A Laplace transform certified reduced basis method; application to the heat equation and wave equation," *Comptes Rendus Math.*, vol. 349, no. 7–8, pp. 401–405, Apr. 2011.
- [61] A. F. Barannyk, T. A. Barannyk, and I. I. Yuryk, "Generalized Separation of Variables for Nonlinear Equation," *Reports Math. Phys.*, vol. 71, no. 1, pp. 1–13, Feb. 2013.
- [62] R. Mahamud and C. Park, "Spatial-resolution, lumped-capacitance thermal model for cylindrical Li-ion batteries under high Biot number conditions," *Appl. Math. Model.*, vol. 37, no. 5, pp. 2787–2801, Mar. 2013.
- [63] G. Guo, B. Long, B. Cheng, S. Zhou, P. Xu, and B. Cao, "Three-dimensional thermal finite element modeling of lithium-ion battery in thermal abuse application," *J. Power Sources*, vol. 195, no. 8, pp. 2393–2398, Apr. 2010.
- [64] M. Al Sakka, H. Gualous, J. Van Mierlo, and H. Culcu, "Thermal modeling and heat management of supercapacitor modules for vehicle applications," *J. Power Sources*, vol. 194, no. 2, pp. 581–587, Dec. 2009.
- [65] J. E. Soc, J. The, E. Society, P. A. Flowers, G. Mamantov, T. Journal, J. H. Taylor, W. S. Benedict, J. Strong, J. Chem, M. Doyle, T. F. Fuller, and J. Newman, "Modeling of Galvanostatic Charge and Discharge of the Lithium / Polymer / Insertion Cell," vol. 140, no. 6, pp. 1526–1533, 1993.
- [66] K. Lee, K. Smith, and G. Kim, "A Three-Dimensional Thermal-Electrochemical Coupled Model for Spirally Wound Large-Format Lithium-Ion Batteries (Presentation), NREL (National Renewable Energy Laboratory)," *Sp. Power Work. Los Angeles, CA*, 2011.
- [67] A. Jarrett and I. Y. Kim, "Design optimization of electric vehicle battery cooling plates for thermal performance," *J. Power Sources*, vol. 196, no. 23, pp. 10359–10368, Dec. 2011.
- [68] J. P. Holman, *Heat Transfer*, Mc Graw Hi. 2002.
- [69] E. Pawlikowski, J. N. D. Bernardi, "A general energy balance for battery systems," *J. Electrochem. Soc.*, vol. 132, no. 5, pp. 5–12, 1985.
- [70] N. Omar, M. Daowd, P. Van Den Bossche, O. Hegazy, J. Smekens, T. Coosemans, and J. Van Mierlo, "Rechargeable Energy Storage Systems for Plug-in Hybrid Electric Vehicles—Assessment of Electrical Characteristics," *Energies*, vol. 5, no. 12, pp. 2952–2988, Aug. 2012.
- [71] N. Omar, M. Daowd, O. Hegazy, M. Al Sakka, T. Coosemans, P. Van den Bossche, and J. Van Mierlo, "Assessment of lithium-ion capacitor for using in battery electric vehicle and hybrid electric vehicle applications," *Electrochim. Acta*, vol. 86, pp. 305–315, Dec. 2012.

[72] V. Pop, H. J. Bergveld, P. H. L. Notten, J. H. G. Op het Veld, and P. P. L. Regtien, "Accuracy analysis of the State-of-Charge and remaining run-time determination for lithium-ion batteries," *Measurement*, vol. 42, no. 8, pp. 1131–1138, Oct. 2009.